Cristina Rossi, CID: 00702784

How do humans learn stable locomotion?

KinnyFinal report 2015.

Table of Contents

Abstract

Investigating the process of learning in human is an ongoing area of research. Many of the sensorimotor dynamics involved in learning movements remain unknown. The aim of this project is to investigate how people learn stable locomotion. To this extent, a virtual reality is created, in which a person runs. A user can interfere with this virtual reality by the means of an haptic interface, through which they modify parameters of the kinematics of running. The virtual reality is rendered to the user through visual and haptic feedbacks. The first part of this project is aimed to designing a system of virtual reality and haptic coupling with the user which enhances the learning and control of (virtual) locomotion in a meaningful way. To this extent, the report contains detailed review of possible haptic couplings and possible locomotion models. A successful system was developed. The second part of this project consists of testing the system and analysing data on how subjects learn to control locomotion. Patterns of input strategies repeated across users are found.

Word count: 16100

1 Introduction

The aim of this project is to investigate how humans learn and control stable locomotion. This aim can be separated into two separate goals:

1. Goal 1: to implement the system of Figure 1.1 successfully, in a way which would allow people to interact with the locomotion model.
2. Goal 2: to investigate how people control and learn to control locomotion, by finding possible patterns and/or key features.

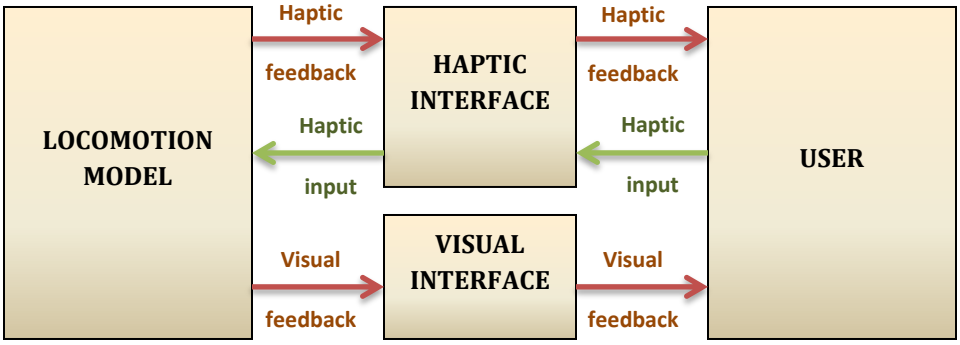

Figure 1.1: overview of the full system to design.

To investigate the control of walking and running, a virtual reality in which a person is running is to be developed. The virtual running has to be controllable through some interface by test subjects, so that data can be collected on how the virtual running is controlled. In Figure 1.1, the 'locomotion model' block is responsible for the equation of motions controlling the virtual runner. Haptic and visual feedbacks, mediated by a grip (handle) and a screen, are responsible for mediating information from the virtual reality to the user. Finally, the haptic interface mediates the input, meaning some action the user takes in the real world which will affect the kinematics of the virtual runner. The first part of this report is dedicated to exploring possible solutions and implementations for the different blocks of the system shown above. Given the availability of the Novint Falcon haptic interface, the haptic interaction is between the virtual system and the upper limb of the user.

The second part of the report is aimed at using the system designed to investigate how people control and learn to control the locomotion system. Tests are carried out on subjects while they try to change some kinematics of the locomotion system. Data on their input and outcome of this are analysed to explore the process of learning. Analysis is carried out with the goal of finding key features necessary for learning and/or control (for example, a particular somatosensory or proprioceptive feedback essential for the learning process), and patterns of learning (for example, specific ways the input is delivered to the system). The system is therefore designed is a way which is likely to give testing results relative to learning locomotion.

Investigating the process of learning in human is an ongoing are of research. Many of the sensorimotor dynamics involved in learning movements remain unknown. Among the several possible applications that knowledge of learning could have, this report focuses on the advancements of lower limb exoskeletons. Exoskeletons have progress a lot in the last few years, but a lot of progress is still needed to enhance the smoothness of the patient locomotion. Current exoskeletons are analysed in **Section 2.4**. As this project analyses how humans control locomotion at low level, if good results are obtained, they could serve as a solid base for improvement of the control of lower limb exoskeletons.

Section 2 of the report explores the background literature of notions needed to design the system of Figure 1.1. Sensory integration in children learning to walk is examined, and a parallel is drawn with the possible haptic feedbacks delivered to enhance the virtual reality experience. Second, a literature review of the possible locomotion models to be used is carried out, and a parallel drawn between ideal models, realistic models and finally real exoskeletons.

Information from Section 2 is used in the following part of the report (Section 3) to design the virtual reality system. A locomotion model, visual feedback and testing set up are developed, and a brain storming of possible haptic coupling (input-output) is reported. Details on peculiar part of the code implementation are also given.

Section 5 presents the testing procedures and results. Preliminary results are carried to select 3 best possible haptic coupling options. Extensive testing is carried out on these 3 coupling options. Results on performance, learning and control strategies are analysed in section 6. Finally, section 7 evaluates the successes and unsuccesses of this project and suggests how to continue future research in the field.

2 Review of background literature

2.1 Integration of sensory information in locomotion

Learning stable and smooth locomotion is a complex task, which requires several years to achieve, and necessitates complex sensorimotor integration. Several attempts have been carried out in literature to investigate the learning process of locomotion, and the importance of the different sensory information in achieving stability. Bril and Ledebt (1998) analyses the findings in the field, as summarised in this section.

While the average child takes their first step soon after their first year of age, it is not until they are 7-8 years old that their walking is comparable to that of an adult. The child has to learn to produce the correct forces, not only in the lower limbs but also in the rest of the body to achieve a successful posture. In the first ca. 5 months after their first independent steps, children experiment with a variety of values and combinations of the different locomotion parameters (such as speed, frequency, length and width of steps, lateral and vertical acceleration of the centre of mass, relative duration of the double support phase -when both feet touch the ground-). After this period, the gait parameters of the child evolve in a smoother way towards the more stable adult gait parameters.

Sensory integration is a determining factor in stable locomotion. Four systems contribute to the necessary information: the visual and somatosensory systems mediate information on the environment, the vestibular and proprioceptive systems enable sensing the relative state (position, angle) of individual body parts, and the position and acceleration of the body with respect to the environment, as well as gravity (Schmuckler, 1990; Pozzo et al., 1998; Ayres, 1972, Ch.2). Studies have shown that the sensory integration evolves as the child learns to walk, and that at different stages of the learning process certain information might be more important than other, but that integration of all these sensory information is necessary to achieve the adult gait (Schmuckler, 1990). In particular, studies have proven the predominance in use of visual information in the first stages of walking, and the essentiality of the vestibular responses (in particular of the otolith system which detects vertical –and roll plane- linear acceleration) for the learning process (Wiener-Vacher et al., 1996).

2.2 Visual and haptic feedback

As discussed in **Section 2.1**, healthy subjects use sensory integration from vision, skin receptors, proprioceptors and vestibular system to achieve smooth locomotion. When it comes to moving in a virtual world, several studies have indicated how artificially combining different types of sensory feedback enhance the realism of the user's experience and improve their performance. In the same way, delivering a combination of sensorial feedbacks can aid a patient using an exoskeleton (Hale and Stanney, 2004; ref). In this section, visual and in particular haptic feedbacks will be discussed.

Visual feedback is consists of the information mediated by the visual system (starting from the retina in the eye) to the central nervous system. As patient with paralysis do not normally have visual system impairments, natural visual feedback from the environment is provided to exoskeleton users. Virtual visual feedback consists of information artificially shown to a user through a screen (or else); it is used to deliver a virtual reality experience, for the purposes of rehabilitation, experiments or gaming.

Haptic feedback is mediated by the somatosensory and proprioceptive systems, delivering respectively tactile and kinaesthetic perception (Hale and Stanney, 2004; Feygin et al., 2002). Tactile perception includes

information that can be deduced by the sense of touch alone, such as texture and 2D shape characteristics; kinaesthetic perception mediates information on the position and movement of an object or part of it. The combination of the two senses allows awareness of 3D shape characteristics. In particular, it is important to note that haptic feedback allows a person to know their body and body parts position, velocity and acceleration, and to know the tension and force in muscles. Several people with lower limb paralysis have lost somatosensory information in the area of the injury. For example, about 45% of spinal cord injuries in the USA are complete, meaning the loss of touch (Spinal Cord Injury Information Pages; Foundation for Spinal Cord Injury Prevention, Care & Cure, 2009).

Virtual haptic feedback is mediated by haptic interfaces, devices which have a grip to which the user holds on to interact with the computer; these same devices can also read haptic input from the user. Haptic interfaces can have one to three degrees of freedom, and can be impedance or admittance devices. An impedance interface outputs force to the user, while reads as input the position of the grip (or its velocity or acceleration); and admittance device outputs a constrained grip position (or velocity or acceleration) to the user, reading as input the force the user exerts on the grip (Hogan, 1985, Part I; Hogan and Buerger, 2005, Ch.19).

Adding haptic to visual feedback has proven a successful strategy for learning new tasks several times in literature (Hale and Stanney, 2004; Morris et al., 2007; Feygin et al., 2002; Sigrist et al., 2014). Several haptic feedback strategies have been explored for training. As explored by Marchal-Crespo and Reinkensmeyer (2009), Sigrist et al. (2012), Powell and O'Malley (2011), the simplest strategy is strict guidance, which output guides the human to follow the specific successful trajectory to achieve the goal; this strategy has though revealed unsuccessful in allowing users to learn to the maximum of their capabilities, as it reduces the activity in the motor pathway of the user. Other guidance strategies, in which the user needs to move autonomously in order to succeed the task, have shown more successful, even though their effectiveness is still disputed. These strategies consist usually of providing assistance only when needed, that is, applying feedback correction only when the user leaves a certain region of tolerance (Marchal-Crespo et al., 2010; Vallery et al., 2009; Sigrist et al., 2014; Rauter et al., 2010), and might include adaptive algorithms (Marchal-Crespo et al., 2012; Ronsse et al., 2011; Krebs et al., 2003); the region of tolerance corresponds usually to a safety or stability boundary.

The most successful strategies have shown to take a step further from guidance. Several temporal separation strategies have proven efficacious, in which the user is first guided through the correct movement, and they then repeat it with no guidance, or alternatively in which the guidance is provided intermittently, at frequencies or about 1Hz (Morris et al., 2007; Feygin et al., 2002; Powell and O'Malley; 2011). Similarly spatial separation, where the guidance is applied to a part of the body different than the one that will be performing the movement, has been explored. Gross resistance strategies which create disturbances for the user have shown a steeper learning curve. These include amplifying the user error, through a constant or proportional diverging force field which activates when the user leaves a tolerance area in the trajectory, and outputting through the interface random noises (Powell and O'Malley, 2011; Marchal-Crespo and Reinkensmeyer, 2009).

While haptic feedback has been widely used to teach the user to reproduce trajectory and forces, there are fewer papers analysing learning of more complex tasks. Hale and Stanney (2004) suggest that haptic feedback which enhances realism, by reproducing the environment input to the somatosensory and proprioceptive systems, enhance the performance of the user. In particular, referring to locomotion, the kinaesthetic

sensation in the lower limbs plays a crucial role and can be reproduced by the haptic device by emulating characteristics of the body motion pattern in walking.

2.3 Modelling locomotion: the SLIP model

Many attempts have been carried out in history to model the biomechanics of the human leg during walking, running and jumping. While several complex models are present in literature, the SLIP (spring loaded inverted pendulum) model is vastly used because it is simple, self-stabilising, and accurate in predicting the centre of body mass trajectory (Hutter et al., 2010, B). The model was introduced by Blickhan (1989), and was widely analysed and used since.

As the SLIP model had been introduced in my Interim Report, the entire section 2.3 (including subsections 1 and 2) is based on the introduction presented in this report; this has been nearly completely re-elaborated and additional notions added, but (parts of) paragraphs / figures captions might coincide with the Interim Report version.

The SLIP model, for running, is shown in **Figure 2.1**. It consists of a point mass fixed onto a spring. The mass, m, consists of the whole body mass, and its position coincides with the centre of mass of the person. The spring of stiffness k_{LEG} and rest length l_0 models the leg currently withstanding the body weight. The SLIP model is originally used to model running and jumping (and only later extended to walking, as it is discussed in **Section 2.3.1**). These bouncing motions consist of two alternating phases: contact phase, where the foot (here, the spring) is touching the ground, and a flight phase, where the body is in free fall. For running, the point mass has both a vertical and horizontal velocity, and the spring is at some angle wrt the ground; for hopping the mass has only vertical velocity, and the spring in vertically placed. Henceforward in this report, the SLIP model will refer to running unless otherwise specified. During contact phase, the foot of the spring is as hinged to the floor, allowing rotation but not horizontal slip; here the angle of the spring is therefore constricted by the equations of motion of the mass. Before landing, the angle of the spring is set to some value α_0, also called 'angle of attack'; the value of the parameter is explored in **Section 2.3.1**.

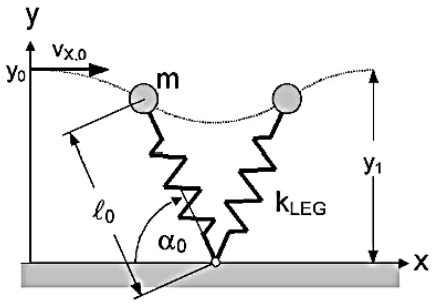

Figure 2.1: SLIP leg model for hopping/running. The parameters are: m=body mass, k=leg (spring) stiffness, l_0=length of leg (spring) at rest, α_0=angle of attack (ie landing). The x,y coordinate system indicates the horizontal and vertical position of the mass, with y_0 being the height at the apex of the flight phase and y_1 the height at landing; $v_{x,0}$ indicates the horizontal velocity at the apex of the flight phase. (Figure taken from: Seyfarth et al., 2002).

The state of the system is defined by the four variables of horizontal and vertical position and velocity. The parameters of the model are: spring (leg) stiffness, body mass, length of the spring (leg) at rest, angle of attack. Further constraints of the system are defined by the initial state of the system. The equations of motion are specified by Blickhan, 1989 to be:

Contact phase:

$$\ddot{x} = \tilde{x}\,\frac{k}{m}\left(\frac{l_0}{\sqrt{\tilde{x}^2+y^2}} - 1\right) \qquad (2.1)$$

$$\ddot{y} = y\,\frac{k}{m}\left(\frac{l_0}{\sqrt{\tilde{x}^2+y^2}} - 1\right) - g \qquad (2.2)$$

Flight phase:

$$\ddot{x} = 0 \qquad (2.3)$$

$$\ddot{y} = -g \qquad (2.4)$$

x,y: Cartesian coordinates of the mass,
$\tilde{x}$: x coordinate shifted such that $\tilde{x} = 0$ is at the point of contact of the foot with the ground,
k: spring stiffness,
m: body mass,
l_0: length of the spring at rest,
g: Earth gravitational acceleration,
α_0: landing angle.

The conditions for changing phase are: (Seyfarth et al., 2002).

Landing for: $y = l_0 \sin\alpha_0$. (2.5)

Take-off for: $\sqrt{\tilde{x}^2 + y^2} = l_0$. (2.6)

The SLIP model illustrated is energy conservative. For certain parameters and initial conditions, which will be explored in **Section 2.3.1**, the trajectory of the mass is periodic (with one period being one flight phase plus one contact phase), and the system is locally stable (meaning it can withstand small perturbations in parameters or initial conditions, and will still converge to the stable periodic trajectory). **Figure 2.2** shows the shape of the mass trajectory, and vertical and horizontal ground reaction forces, for stable periodic locomotion.

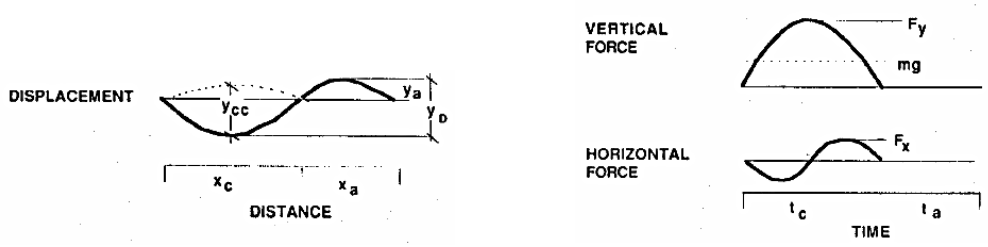

Figure 2.2: plots showing, for stable periodic locomotion, the general shape of: mass trajectory in the x,y plane (left), vertical ground reaction force in time (top right), horizontal ground reaction force in time (bottom right). x_C and t_C indicate the space and time of the contact phase, x_A and t_A indicate the space and time of the aerial (flight) phase. (Figure taken from: Blickhan, 1989).

2.3.1 Investigating the stability of the SLIP model

The stability of the SLIP model has been investigated several times in literature (Seyfarth and Geyer, 2002; Geyer et al., 2005; Seyfarth et al., 2002; Lipfert et al., 2011; Blickhan, 1989). Given the proper choice of parameters, stability can be achieved for any jump height (Seyfarth and Geyer, 2002) or target speed. In this section, the stability analysis provided by Seyfarth et al. (2002) is explored, which relates stability to speed.

As previously mentioned, the model stability depends on its parameters and initial state; the system is considered stable if the mass trajectory is periodic and locally attractive. It can be seen whether the mass trajectory is periodic by comparing two subsequent strides: if there exist two points belonging to the two strides with same physical conditions, then the leg movement will repeat periodically. Choosing the apex (zero vertical velocity) of the stride as the point to analyse, the trajectory will be periodic if the mass at the apexes in the two consequent strides has in both same height and horizontal velocity. It should be noted than in an ideal model, where energy is conserved, equal apex height implies equal horizontal velocity.

Local stability analysis is necessary to ensure the real model is resilient to small disturbances. Calling y_i the height of the apex of stride i, and i+1 the subsequent stride, a graph y_{i+1} vs y_i can be plotted given the model parameters and the horizontal velocity of the mass at apex y_i. A mass trajectory is periodic (for some parameters and initial conditions) for an initial apex height $y_i = Y_0$ if this leads to $y_{i+1} = y_i = Y_0$. A stable system is then achieved for some SLIP parameters and initial conditions if the slope of the graph y_{i+1} vs y_i at the fixed point ($y_{i+1} = y_i = Y_0$) is between [-1,1]; this correspond to the fixed point being locally attractive, as for a small perturbation in apex value y_i , the following y_{i+1} height counterbalances this error. A sample plot of y_{i+1}vs y_i for specific parameter/initial values is shown in **Figure 2.3**; the plot also illustrates the method for finding the fixed points and checking their stability.

Plots illustrating the stability of the system given different parameters and initial conditions are shown in **Figure 2.4**. The stability is expressed in terms of number of strides ran before falling; simulations of the SLIP model were carried out by the author using MATLAB ode113. Real life observations were then compared to the data obtained. The mass was kept fixed to 80Kg throughout the simulations; when comparing this data to real life observations the stiffness value was scaled to this mass value, as the leg kinematics do not change for different masses if the eigenfrequency ($\sqrt{k/m}$) doesn't change. The stability curve of k_{leg} (leg stiffness) vs. α_0 (angle of attack) for initial horizontal velocity 5m/s is:

$$k_{leg} = \frac{1600}{1 - \sin(\alpha_0)} \qquad (2.7)$$

Several attempts appear in history to extend the model to walking, which is naturally less stable than running. Parameters can be found to achieve stable locomotion at specific speeds such as 1.04 m/s and 1.55 m/s, but not for the whole range of walking speeds (Lipfert et al., 2011). Adding complexity to the model, by considering the limb as multi-unit, greatly expands the achievable stable speeds (Hutter et al., 2010, B); SLIP principles still hold in this modified model.

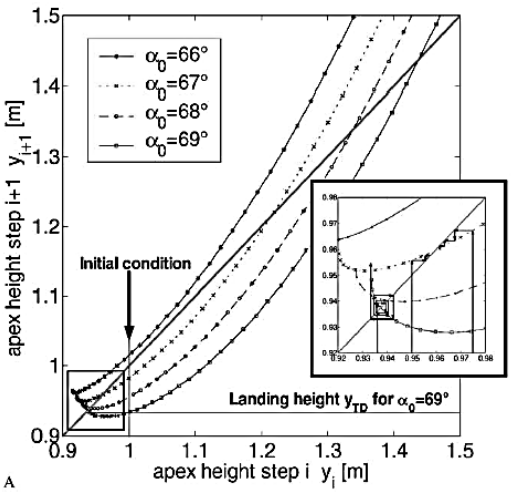

Figure 2.3: y_{i+1}vs y_i plot (y = apex height, i = stride) for horizontal velocity at apex = 5m/s, leg stiffness = 20kN/m, leg length = 1m, mass = 80Kg, and angles of attack (curves from top to bottom) of 66°, 67°, 68° 69°. The straight line of slope 1 crosses the curves at the fixed points (where $y_{i+1} = y_i$). It can be seen graphically whether the tangents to the curves at these fixed points are less or more steep than the slope 1 straight line, indicating respectively that the fixed point is stable or not. In the case shown above, the lower intersections with the α_0= 67°, 68° curves are stable fixed points, for which a stable motion is achieved (given the parameters/initial condition indicated). (Figure taken from: Seyfarth et al., 2002).

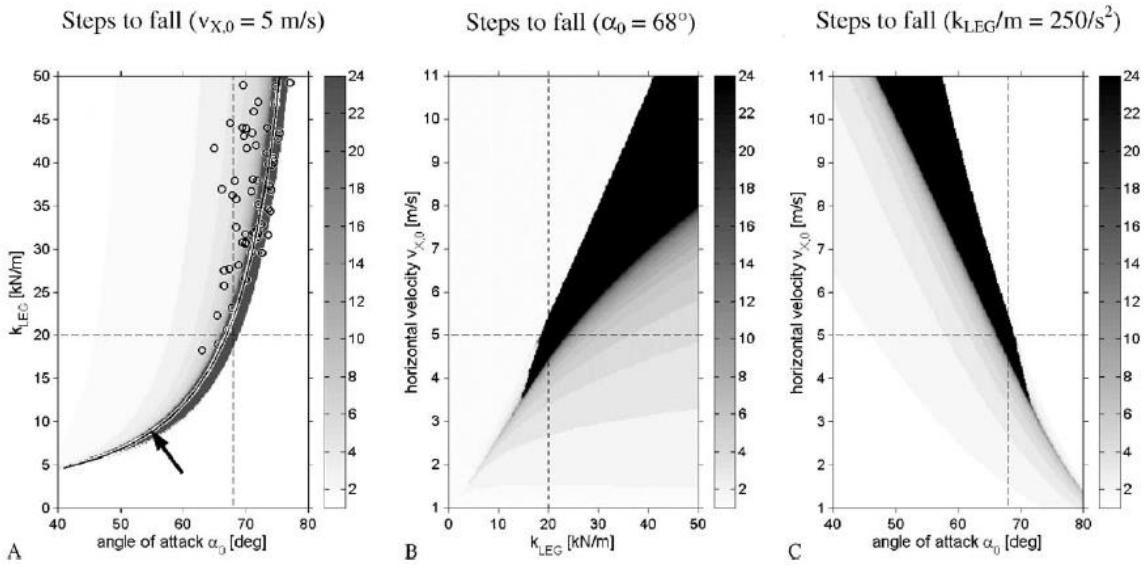

Figure 2.4: stability of the SLIP model when varying 2 parameters. The color map at the right of the individual plots relates the shade of the plot to the stability of the model in terms of strides ran before falling; the maximum number of strides was set to 24. All plots are for a body mass of 80Kg, initial position at apex of height y_0=1m, length of leg at rest l_0=1m. Left: given initial horizontal velocity of 5m/s, the stable region in the stiffness vs angle of attack graph resembles a J. Small circles are plotted from experimental observation of people of different mass running; the stiffness was scaled to 80Kg mass keeping $\sqrt{k/m}$ constant. Middle: for an angle of attack of 68°, it can be seen that as the horizontal velocity is increased, the leg stiffness needs to be increased as well in order to achieve stability. It is also not possible to be stable given a fixed angle of attack for too low velocity or stiffness. Right: for leg stiffness = 20kN/m, it can be seen that as the horizontal velocity is increased, the angle of attack needs to be decreased. For a fixed stiffness/mass ratio is also not possible to achieve stability for too low velocity or too high angle of attack. (Figure taken from: Seyfarth et al., 2002).

2.3.2 Locomotion on realistic surfaces

Until now, locomotion on an ideal surface (infinitely stiff, flat and even) was analysed. The SLIP model has been proven stable (for certain parameters) for running on several more realistic surfaces. Ferris and Farley (1997), Ferris et al. (1998) and Farley et al. (1998) investigate the leg stiffness adjustment consequent to hopping (or running) on surfaces of different stiffness. A plot of leg stiffness vs. surface stiffness is shown in **Figure 2.5**. It was shown experimentally that humans and animals compensate the change in surface stiffness so that total vertical stiffness of the system remains about constant; the total vertical stiffness of the system was calculated to be $k_{tot} = \frac{F_{peak}}{\Delta y_{peak}}$ (2.8), where F_{peak} is the maximum ground reaction force (equal to the force acting through the spring), which happens at the maximum length displacement Δy_{peak} (Ferris and Farley, 1997). This allows the kinematics of the locomotion (horizontal velocity and ground contact time) to remain unchanged between different surfaces.

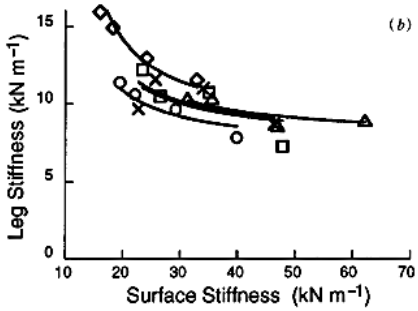

Figure 2.5: plot of leg stiffness vs surface stiffness. The data was recorded experimentally in subjects running on surfaces of different stiffness. Different symbols indicate data for different subjects. (Figure taken from: Ferris et al., 1998).

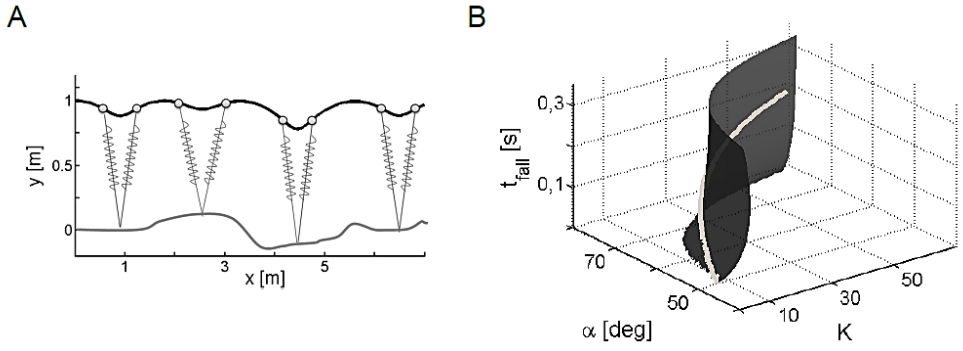

Figure 2.6: illustration of the SLIP system travelling on an uneven ground (A) and the surface of stability of parameters α (angle of attack) and K (leg stiffness) as a function of t_{fall} (time from apex of flight to landing) (B), for normalised speed $F = \frac{v^2}{gL} = 2.25$, where g is gravity, L is leg length at rest, v is horizontal velocity of flight phase (4.7m/s for L=1m). The white curve on (B) represents a possible choice of parameter adaptation. (Figure taken from: Ernst et al., 2009).

Hutter et al. (2010, A), Hutter et al. (2010, B) and Ernst et al. (2009) investigate the stability of the system on uneven surfaces, as illustrated in **Figure 2.6a**. No fixed parameters are generally found for the SLIP model to run stable at a constant speed, but several simple control strategies exist to modify parameters as the ground level change, allowing periodic stable locomotion. Strategies which only make use of internal states of the system exist (without the need to know the ground heights); as these states are measurable, this enables real systems to be automated to achieve stability. Parameters values that achieve stable locomotion given the fall time (time from apex to landing) are explored by Ernst et al. (2009), and presented in **Figure 2.6b**. Hutter et al. (2010, A) provides the basis for parameter estimation using contact time.

A special case of uneven ground is a smooth sloped ground. For this type of surface, angle of attacks can be found so that the SLIP model is stable with no external control, as shown by Garcia et al. (1998).

2.3.3 Real life SLIP system

The basic SLIP model has been adapted to more realistic systems in several papers (Altendorfer et al., 2004; Hutter et al., 2010, B; Peuker et al., 2012; Farley et al., 1998). Variations to the classical system include: considering the leg as a multi-unit system, accounting for the mass of the leg, modelling the hip, knee and ankle joints (as rotational spring or spring plus dumper, often with the addition of actuators), considering bipedal locomotion, accounting for the energy dissipation in joint and/or contractile elements, and often a combination of these. As real joints and contractile units, in the human body and even more in an exoskeleton, have some degree of dumping, actuators are necessary to compensate for energy loss; actuators are also used to increase stability of the system to real world disturbances.

2.4 Locomotion exoskeletons: state of art

There are few lower limb exoskeletons are available on the market, and other in the late stage on their research. As discussed by Gwynne (2013), the devices interface one of the three possible hierarchical levels of control. At the high end, the patient only controls the intention to move, and the device will perform the walking autonomously, while also maintaining the patient's balance. This is the strategy adopted by the REX (rexbionics.com), where the patient controls the walking onset and direction with a hand joystick. At a medium level, the patient can control the onset of individual steps, while maintaining their balance with crutches. To this category belong most devices, such as the Ekso (eksobionics.com) and the ReWalk (rewalk.com); the onset on the step is trigger either by a button, or by patient leaning forward with their upper body. At the lowest level, the patient controls (part of) the actual lower limb movements occurring during each step. At the moment, to this category belong only assistive devices which help patients with difficulties in locomotion but not complete paralysis; the patient perform the action of stepping autonomously and the device assists in the critical phases of the step (Ronsse et al., 2011). These devices are meant for permanent locomotion assistance or, more often, for rehabilitation. EMG (electromyography) can also be used to detect the appropriate guidance needed (Carpi and De Rossi, 2006, Ch. 3.1; Krebs et al., 2003). While there is no into EEG (electroencephalography) controlled exoskeleton available on the market yet, ongoing research in the field has shown successful results. Kilicarslan et al. (2013) are working on NeuroRex, a development of REX which uses EEG (instead of the joystick) to detect the user's intention to move and in which direction; preliminary tests with a test subject have shown successful. Contreras-Vidal et al. (2012) have successfully decoded from EEG signal lower limb joints movement during locomotion; this could extend in the future the low level control of locomotion (which offers more freedom of movement) to less able patients.

3 Design

An overview of the full system designed was presented in Section 1, and is here proposed again in Figure 3.1. Investigating the learning and control of locomotion is achieved by simulating the process in a virtual environment. The virtual environment consists of a body continuously performing the action of running. The kinematics of running are dictated by the equations of the locomotion model chosen; in particular the model must include a way for the haptic input from the user to change the kinematics of the locomotion.

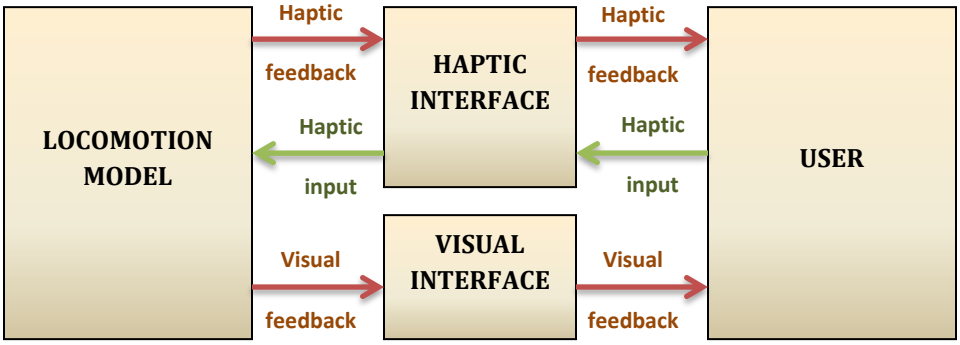

Figure 3.1: overview of the full system to design.

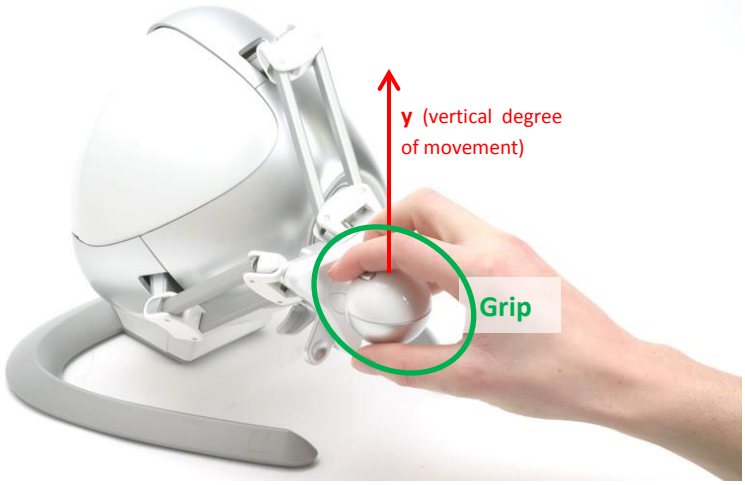

Figure 3.2: Novint Falcon haptic interface. The grip of the device, and the vertical degree of freedom, are indicated. (Figure taken from: bit-tech.net).

Interaction between the user and the virtual reality is mediated by visual and haptic interfaces. The visual interface used was the 15.6 inches screen of a HP G62 notebook. The haptic interface used in the Novint Falcon (novint.com), a 3-degree of movement impedance device, shown in **Figure 3.2**. The user interacts with the haptic device through a spherical end called 'grip'. Only one degree of movement (the vertical, as shown in the figure) of the device is used in this project.

Both visual and haptic interface provide 'feedback' to the user, information about the system running in the virtual reality. The purpose of using feedback is to facilitate the user in learning and controlling the locomotion system. Feedback which delivers information which a real runner would actually use in reality, is likely to be more successful and at the same time provide more useful information for the investigation of the learning process. These two keys were used as fundamentals when designing feedback. The haptic interface is also the medium of 'input', the active interaction which allows the user to change the kinematics of the running system. The following subsections analyse in detail the design of the different blocks of the system of **Figure 3.1**.

3.1 Locomotion model

The design of the locomotion model was based on the SLIP model analysed in **Section 2.3**. In addition to the classical model expressed by **equations 2.1 to 2.5**, other means of input, and realistic adaptations, were considered.

The complex leg model analysed by Van Soest et al. (1985), consisted of 3 inputs points located at the hip, knee and ankle joints. Comparing knowledge of this model with biomechanics and the running SLIP model, and considering that:

- In flight phase, (nearly) only gravity is interacting with the body, so the trajectory of the centre of mass is not modified compared to the standard SLIP
- In contact phase, the foot in contact with the ground can be considered as a pivot, the only medium for external forces interaction (other than gravity)

the action of input torques at the joints on the SLIP model can be summarised as following:

- During flight, the combined torque at the joints can result in changing the angle of attack and length of the leg at landing
- During contact, the combined torque at the joints can result in changing the leg stiffness / applying force aligned with the spring to the upper body, and in applying a torque at the pivot point.

The complete model, which takes into account these inputs, is shown in **Figure 3.3a**. The mass represent the body mass located at the centre of mass, the spring represents the leg. It should be noted that applying force aligned with the spring can be replaced by changing the spring stiffness (and vice versa), as the total force on the mass (in the direction of the spring) is $F_{tot} = k(l_0 - l) + F_{input}$, so there always exists a value of k during contact which results the same kinematics as applying some desired input force. The equations for this model are:

Coordinate equivalence:

$$r = \sqrt{\tilde{x}^2 + y^2} \qquad (3.1)$$

$$\theta = \tan^{-1}\frac{\tilde{x}}{y} \quad (3.2)$$

$$\tilde{x} = r\sin\theta \quad (3.3)$$

$$y = r\cos\theta \quad (3.4)$$

θ: angle if the spring from the y axis,
T: input torque at hinge,
m: body mass,
r: leg length,
g: Earth gravitational acceleration,
F: input radial force acting on mass,
k: spring leg stiffness,
r_0: length of spring at rest,
θ_0: angle of attack (angle of the leg at landing)
x,y: Cartesian coordinates of the mass (m),
$\tilde{x} = x - \Delta x$: coordinate shifted such that $\tilde{x} = 0$ is at the point of contact of the foot with the ground (m).

Contact phase:

$$\ddot{\theta} = \frac{T}{m} + r\ g\ \sin\theta \quad (3.5)$$

$$\ddot{r} = \frac{F}{m} - g\ \cos\theta - \frac{k}{m}\ (r - r_0) \quad (3.6)$$

Flight phase:

$$\ddot{x} = 0 \quad (3.7)$$

$$\ddot{y} = -g \quad (3.8)$$

$$\theta_0 \leftarrow input \quad (3.9)$$

$$r_0 \leftarrow input \quad (3.10)$$

Phase changes:

landing for $y = r_0\ \cos\theta_0$, (3.11)

take-off for $r = r_0$. (3.12)

The update of the dummy variable Δx happens at the start of each contact phase:

$$\Delta x\ = x\ (t_{contact}) + r_0 \sin\theta_0. \quad (3.13)$$

Where $x\ (t_{contact})$ is the value of x at the first contact time.

Preliminary results on user tests using the simpler SLIP model, discussed in Section 5, showed the difficulty in controlling the system given the little training time available. The use of this complex model was therefore dropped and will be discussed in the Conclusions Section. The standard SLIP model with stiffness as the only input was used. The force input was maintained for certain tests as an alternative to inputting stiffness. The fact that runners can adjust their angle of attack during flight phase was used in some coupling strategies, but not as a standalone input. Coupling strategies are discussed in depth in Section 3.

Realism was added to the standard SLIP model by adding air drag, dumping across the spring, and by modelling the ground as spring-dumper system. The final system used is shown in **Figure 3.3b**.

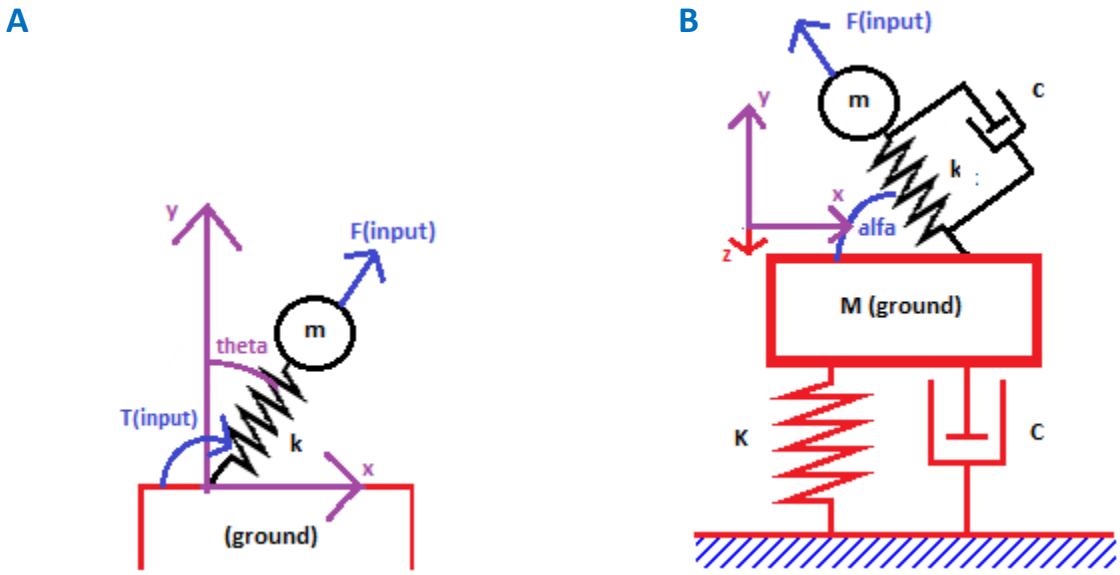

Figure3.3: ideal locomotion model with input torque and force (left), and realistic locomotion model with input force on variable stiffness ground (right).

The equations of motion are:

Contact phase:

$$\ddot{x} = \frac{\tilde{x}}{l}\frac{F_r}{m} \tag{3.14}$$

$$\ddot{y} = \frac{y-z}{l}\frac{F_r}{m} - g \tag{3.15}$$

$$\ddot{z} = -\frac{y-z}{l}\frac{F_r}{M} - \dot{y}\frac{C}{M} - y\frac{K}{M} - g \tag{3.16}$$

With:

$$(\#)\ F_r = k\,(l_0 - l) + F - c\sqrt{\dot{x}^2 + \dot{y}^2} \tag{3.17}$$

Where (#) indicates F=0 for modality input=k.

$$l = \sqrt{\tilde{x}^2 + (y-z)^2} \tag{3.18}$$

Flight phase:

$$\ddot{x} = -c_{air}\dot{x} \tag{3.19}$$

x,y: Cartesian coordinates of the mass (m),
$\tilde{x} = x - \Delta x$: coordinate shifted such that $\tilde{x} = 0$ is at the point of contact of the foot with the ground (m),
k: spring stiffness (N/m),
c: leg dumping (Ns/m),
m: body mass (kg),
l_0: length of the spring at rest (m),
g: Earth gravitational acceleration (m/s^2),
c_{air}: air drag (Ns/m),
α_0: landing angle (rad),
F_r: total force acting on mass in the spring direction (N),
F: input force acting on mass in the spring direction (N),
l: length of the spring (m),
M: ground mass (kg),
K: ground stiffness (N/m),
C: ground damping (Ns/m),
z: ground vertical position (m).

$$\ddot{y} = -g - c_{air}\dot{y} \quad (3.20)$$

$$\ddot{z} = -\dot{y}\,\frac{C}{M} - y\,\frac{K}{M} - g \quad (3.21)$$

$$\alpha_0 = \sin^{-1}\left(-\frac{1600}{k-5000(\dot{x}-5)} + 1\right) \quad (3.22)$$

$$(*)\quad k = 20000 + 5000(\dot{x} - 5) \quad (3.23)$$

Where (*) indicates the equation only holds in modality input=F.

Phase changes:

landing for $y = l_0 \sin\alpha_0$, (3.24)

take-off for $l = l_0$. (3.25)

The update of the dummy variable Δx happens at the start of each contact phase:

$$\Delta x = x\,(t_{contact}) + l_0 \cos\alpha_0. \quad (3.26)$$

Where $x\,(t_{contact})$ is the value of x at the first contact time.

The angle of the leg (spring-dumper) is kept as angle of take-off for the first part of the flight phase (until apex is reach) and is set to α_0 in the second part of flight phase.

Equations 3.22 and 3.23 are explained in **Section 3.1.1**. An important feature of the model used for tests is that, if a parameter (k and α_0) is not read as input, it is automatically adjusted to a stable value. The model parameters and initial conditions are set to:

y(t=0): 1m,	k: 20kN/m,	l_0: 1m,	K: 100kN/m,	$\dot{z}$(t=0): 0.
$\dot{y}$(t=0): 0,	c: 40Ns/m,	c_{air}: 1Ns/m,	C: 100kNs/m,	
x(t=0): -3m,	m: 80kg,	M: 10kg,	z(t=0): 0,	

3.1.1 Stability equations

The stability analysis of the SLIP model, for different values of k, α_0, $\dot{x}$ initial, by Seyfarth et al. (2002) is summarised in **Section 2.3.1**. The aim of this section is to extract, from this analysis, approximate equations of stability governing the relationship between all 3 parameters. Equations which, for a $\dot{x}_{flight}$ value, give the optimal, and limit of stability, k and α_0 are investigated. It should be noted that while the analysis of Seyfarth et al. considered only the initial horizontal velocity, here the horizontal velocity during a flight phase is considered; values of k and α_0 stable for certain $\dot{x}$ initial are taken, by approximation, to be stable for that $\dot{x}$ of any flight phase. This analysis is approximate and carried out purely for functional purpose of the experimental setup; it should not be considered an optimal dead-beat control.

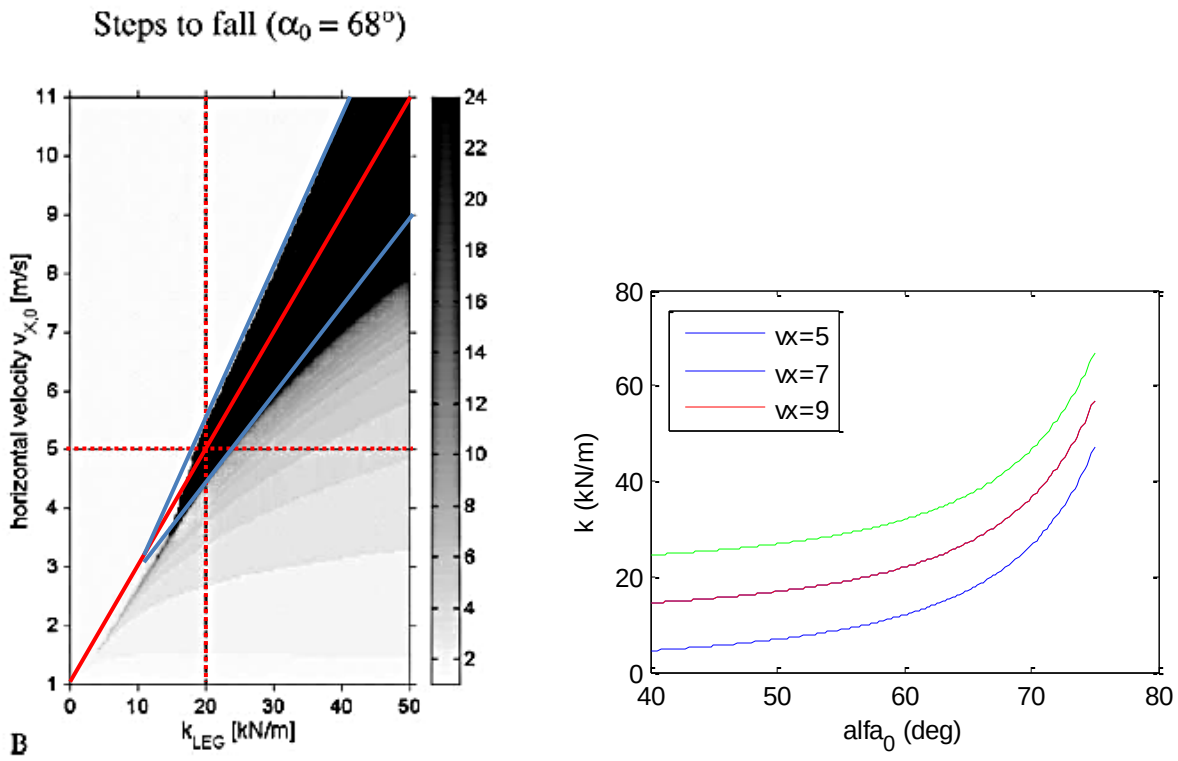

Figure 3.4: stability plots. Stability region of velocity vs. stiffness for constant alpha0 (left) and approximated stability optimality (red) and limits (blue). Stability j-curves of k vs. alpha0 for different value of velocity given Seyfarth et al. formula (blue) and new estimate (red, green). (Left figure taken by Seyfarth et al., 2002)

Figure 3.4 shows stability references drawn on a figure taken by Seyfarth et al. (2002) (left), and the curve of stability k vs. α_0 for $\dot{x}_{flight} = 5m/s$ (blue), which was found to be by Seyfarth et al.:

$$k_{leg} = \frac{1600}{1-\sin(\alpha_0)} \qquad (2.7)$$

The red lines show curves of good stability as they have margins of stability on both higher and lower values. The green lines show the limits of stability.

While keeping a value of $\alpha_0 = 68°$ allows some values of k to be found at all speed ≥ 5m/s that achieve the stability of the system, an improved calculation of the value of α_0, which allow more values of k to result in a stable system, would help the user achieving challenging learning task.

It is observed that, for α_0=68° and for $\dot{x}_{flight} \geq 5m/s$, the stability relation between k and $\dot{x}$ indicated by the red line is:

$$k = 5\dot{x}_{flight} - 5\ \left(\frac{kN}{m}\right) \qquad (3.27)$$

As mentioned above, this stability relationship between k and $\dot{x}_{flight}$ has acceptable margins of tolerance and is therefore used as equation in the model (**Section 3.1**). For $\dot{x}_{flight}$=7, 9, and 11m/s, and α_0=68°, k takes values 30, 40, and 50 kN/m; these values are stemmed on the k vs. α_0 stability plot. According Seyfarth et al., for speeds higher than 5m/s the J-shaped relationship between k and α_0 should shift and enlarge but not change shape. Therefore, an attempt to fit the j-shaped curve to the new k-$\dot{x}_{flight}$ values was made by simply shifting the curve upwards. The equation obtained is:

$$k_{leg} = \frac{1600}{1-\sin\alpha_0} + 1000(5\dot{x}_{flight} - 25) \qquad (3.28)$$

Given this equation, the standard SLIP model was tested in MATLAB for different initial horizontal velocities and different stiffness for constant $\alpha_0 = 68°$ and α_0 obtained by **equation 3.22**. It should be noted that the stability analysis of **Figure 3.4** (left) is based on number of steps to fall and not on the smoothness of the locomotion, while both factors are considered in this analysis. The value given by **3.22** enlarged the stability region of k and therefore it was chosen over the fixed value of 68° (**Section 3.1**). The newly achieved stability range of the stiffness was considered an appropriate region of tolerance for the purpose of the experiment so no further attempt to enlarge the stability region was carried out; the $\dot{x}_{flight}\ vs.\ \alpha_0$ plot of stability in Seyfarth et al. (2002) shows that more stable solutions exist.

An analysis of the stability limits of the stiffness is carried out to the purpose of implementing region-tolerant haptic feedback (see **Section 3.4.1**). To this extent, approximate limits of k within which the system is stable, given a certain speed, are estimated by the Seyfarth et al. (2002) analysis, as shown in **Figure 3.4**. As mentioned above, the region of stability is enlarged by **eq. 3.28** compared to the one shown in the figure, but at the same time the Seyfarth et al. analysis only considered not falling as a success condition, and not the periodicity of the trajectory. Therefore, the limits of stability inferred by the figure can be considered a good approximation of the target region of tolerance. The equations for the lower and upper stiffness bounds, which correspond to the green lines in **Figure 3.4**, are respectively:

$$k_{leg} \geq \frac{11}{3}v - \frac{1}{3}\left(\frac{kN}{m}\right) \qquad (3.29)$$

$$k_{leg} \leq \frac{20}{3}v - 10\left(\frac{kN}{m}\right) \qquad (3.30)$$

3.2 Choice of target for experiments and stability

The goal of the tests carried out in this project is to analyse if and how people can achieve a desired stable locomotion. As mentioned above, the system is created such that it automatically stabilises in most conditions. This is a feasible concept for real life applications as a possible exoskeleton should be design to be as stable as possible for the user. Furthermore, fixing most model factors and isolating an individual task allows studying the user's performance in achieving a very specific goal.

The target of the experiments, for the test subjects, should be therefore to change certain kinematics of the system in the most stable and quick was possible. Speed of locomotion is found to be the most useful variable to control in real life, while other variables such as height, frequency, phase of jumps, or location of the body in time could also be controlled.

Three experiments with increasing difficulty were implemented, whose goal was to match:

1. Target horizontal velocity of flight phase
2. Target horizontal position of the body in time (which is velocity + phase of motion)
3. Target mass trajectory (including all variables mentioned above)

It should be noted that matching a target speed was expressed in terms of matching the horizontal velocity during flight phase, which in constant except for air drag. Given the preliminary results carried out on 1., showing the difficulty of user in achieving the task, 2. and 3. were discarded, and task target 1. will be assumed henceforth in the report.

Therefore the horizontal velocity in flight phase was taken as goal for subject trials. Tolerance of ±0.3m/s of the target speed was allowed. Regarding the choice of stability of the system, the model was considered crashed if the mass touched the ground, the horizontal velocity turned negative, or the mass flew higher than 2 meters. A timeout of two minutes per trial was chosen, while the trial was considered successful after being in the target region and velocity for 10 seconds.

3.3 Visual feedback

Given the two targets defined above, horizontal velocity in flight and vertical region of tolerance, visual feedback was generated with the purpose of illustrating to the user their current and target state. A 2D display showing the SLIP system from an external point of view was developed; which allows the user to have a complete picture of the state of the system. An internal point of view representation was considered but discarded due to the lack of training time of the users and subsequent preliminary results, this is further discussed as **future work**.

A capture of the system visual feedback is shown in **Figure 3.5**. The system was displayed as a line representing the leg (the spring-dumper parallel), and a mass mounted on it. The ground was displayed as a horizontal line. The system travelled horizontally from the left to the right of the screen, when it reached the right end of the screen it was shifted back to the left start. The vertical region of tolerance was indicated by dotted horizontal lines. A flow of dots moving horizontally at the target speed, together with an arrow indicating the direction and magnitude of the needed acceleration, provided feedback on the target horizontal velocity in flight phase. The body mass, usually displayed as red, turned green when moving at the correct horizontal flight velocity (±tolerance) and laying within the vertical tolerance region. After a trial ended, the reason of the completion ('success', 'fallen', or 'timeout') was displayed.

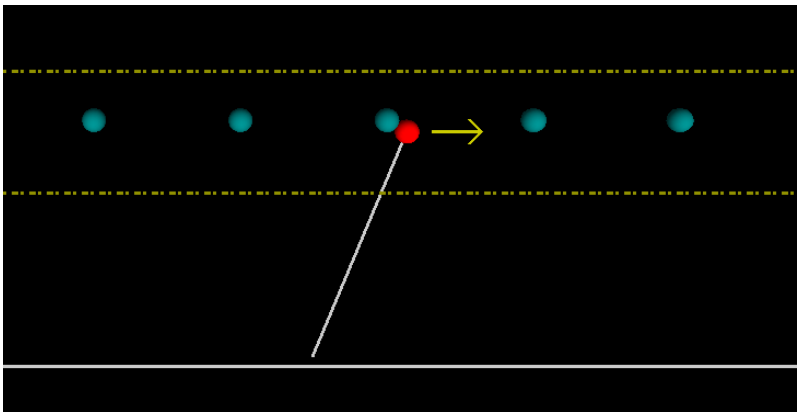

Figure 3.5: capture of the implemented visual feedback.

3.4 Development of a haptic coupling strategy.

Choosing a haptic coupling strategy implies choosing a proper haptic feedback for the system, and a related haptic input. As mentioned in **Section 2.2**, several haptic feedbacks could be found in literature, but not many experiments had been performed on complex learning tasks. In this section, strategies to input to the system (defined by **equations 3.14** to **3.26**) either the value of the leg stiffness or the force, in the direction of the spring, are investigated. The user controls only one input to the system. The interface with the system is the haptic interface Novint Falcon. Only one degree of movement is allowed to the user (the vertical movement), while the other two degrees of freedom are constrained; in the same way the haptic feedbacks discussed in this section only act on the vertical axis of the interface. Each input corresponds therefore to some mapping between the position of the interface grip, and the input stiffness or force. Furthermore, the strategies are developed on an energy conservative system (all dumping in assumed to be zero in analysis), even though dumping is present in the actuation of the coupling; this choice arose by the idea dumping is a disturbance/un-ideality. The reader is reminded that the parameter α_0 is always automatically adjusted to be stable (if possible) given the current stiffness and speed, and the parameter k is automatically adjusted to a stable value when the user controls the force as input.

While this section presents several possible couplings, preliminary tests were used to select the best 3 coupling option to carry out the main tests. Testing methods and results are discussed in **Section 5**.

3.4.1 Possible couplings

Classical strategies such as guidance and error augmentation can be applied to control of stiffness (k). In fact, as analysed in **Section 3.1.1**, for certain flight phase horizontal velocities there are only certain values of the stiffness which would result in a stable system. Given the value of the stiffness to be the input to the system, options for haptic coupling that follow these strategies are:

Common parameters used to define haptic coupling equations are: F_o=output force, F=input force, k_{in}=stiffness input, y_{ref}=some vertical grip position of reference (usually target k and 0 force), y_h=vertical haptic grip position; other variables are system parameters of eq.3.14-26, $\propto$: means proportional.

1. Single point guidance feedback, with linear k input. This strategy consists of guiding the input of k towards an optimal stable value (as calculated by **eq. 3.28**), with a force proportional to the distance from this value. While this strategy has proven unsuccessful for passively teaching, in this coupling the user is required to shift away from the stable stiffness value in order to change the dynamics of the system. The input is a linear mapping of the vertical position of the interface grip to the value of k.
   Equations:
   $F_o \propto (y_{ref} - y_h)\ ;\quad y_{ref} \leftarrow eq.3.28$ (3.31)
   $k_{in} - k(eq.3.28) \propto (y_h - y_{ref})$ (3.32)
   Meaning the deviation of input k from the optimal position is proportional to the deviation of the grip to the reference position.
2. Single point guidance feedback, with incremental k input. In this case, the input is a linear mapping of the grip position to the rate of change of the stiffness. Positions below a nominal 0 rate values will cause the stiffness to continuously decrease, and vice versa. Haptic feedback will guide the user towards increasing or decreasing the stiffness to achieve a more stable value. Alternatively, a simple feedback guiding the user to the zero-rate position is used.
   Equations:
   $F_o \propto (y_{ref} - y_h)\ ;\quad y_{ref} \equiv gain = 0\ or\ gain \propto k_{optimal} - k$ (3.33)
   $gain \propto (y_h - y_{ref})$ (3.34)
   $k = k + gain * \Delta t_{input}$ (3.35)
   With Δt_{input}=time of validity of the input (time of one program iteration)
3. Area of tolerance guidance feedback, with linear k input. This coupling is analogous as the one analysed in 1., with the exception that no haptic feedback is delivered (except for viscosity) if the user is within the region of tolerance of k, and the force feedback when leaving the region is proportional to the distance to the closest region boundary, as defined by **eq. 3.29-30**. The input is as before.
   Equations:
   $$F_o \propto \begin{cases} (y_{refUp} - y_h); & if\ y_h > y_{refUp} \\ (y_{refLow} - y_h); & if\ y_h < y_{refLow} \\ -\dot{y_h}; & otherwise \end{cases} \quad (3.36)$$
   $with\ y_{refLow} \leftarrow eq.3.29; y_{refUp} \leftarrow eq.3.30$
   $k_{in} - k(eq.3.28) \propto (y_h - y_{ref})\ ;\quad y_{ref} \leftarrow eq.3.28$ (3.37)
4. Error augmentation, with linear input k. This strategy consists of applying a force which pushes the user away from the stable stiffness value. As in 3., there is a region of stability tolerance where no haptic feedback is delivered (except for viscosity), and the force outside the region is proportional to the distance from the closest boundary (**eq. 3.29-30**), but the force has now opposite sign. Error augmentation has proven successful in literature, and is analogous to body sensorial information (vestibular and proprioceptive in particular) which alert of the loss of balance.
   Equations:
   $$F_o \propto \begin{cases} -(y_{refUp} - y_h); & if\ y_h > y_{refUp} \\ -(y_{refLow} - y_h); & if\ y_h < y_{refLow} \\ -\dot{y_h}; & otherwise \end{cases} \quad (3.38)$$
   $with\ y_{refLow} \leftarrow eq.3.29; y_{refUp} \leftarrow eq.3.30$
   $k_{in} - k(eq.3.28) \propto (y_h - y_{ref})\ ;\quad y_{ref} \leftarrow eq.3.28$ (3.39)

5. Single point guidance feedback with temporal separation, and linear k input. This consists of the same coupling as in 1., but the feedback is provided intermittently, with a frequency of 1Hz.
   Equations: as 1., but feedback delivered only 1s out of every 2 seconds.

When considering the force as input to the system, haptic coupling strategies have a closer relation to the human sensory integration process and its use in achieving stable and smooth locomotion. In **Section 2.2** it is suggested that information relating to the body position (implying also velocity and acceleration) in space, and well as the force (tension) in involved muscles, enhances the user performance of locomotion in a virtual environment; in real situations this information is delivered by the sensory integration of sight, touch, proprioception and vestibular system, and is important in learning to walk (**Section 2.1**). On these premises the following haptic couplings were theorized for force input:

1. Compression force in the leg muscle as feedback. This is equivalent to the ground reaction force (term F_r of **eq. 3.17**). This feedback couples meaningfully with different possible inputs, which are explored later in this section.
   Equations:
   $F_o \propto -\frac{y-z}{l} * F_r$ (3.40)
   $F \propto \begin{cases} y_h, & or \\ \dot{y}_h, & or \\ \ddot{y}_h & . \end{cases}$ (3.41)
2. Model mass movement as feedback, linear input. This feedback is a strategy for outputting the model acceleration (and movement in general) in a way which is restrained independently of the user action, making the coupling more stable. Outputting the position of the mass in time (scaled) is equivalent to outputting acceleration while assigning a virtual mass to the haptic interface grip. The input is read to be proportional to the vertical displacement of the grip from the (mapped) position of the mass at that instance in time. The output position constrain in achieved by virtual springs, therefore the input is also proportional to the force applied by the user to displace from the outputted trajectory.
   Equations:
   $F_o \propto (y - y_h)$ (3.42)
   $F \propto (y_h - y)$ (3.43)
3. Position of the sole of the foot as feedback, force input. The key feature of this feedback consists of constraining the grip movement to the ground movement during contact phase, which can enhance control if the chosen ground is particularly low stiffness. The input would be the force required to move away from the constrained output, which could realistically be in terms of the spring and dumper components of the ground.
   Equations:
   $F_o \propto K(z - y_h) - C * \dot{y}_h$ (3.44)
   $F \propto K(y_h - z) + C * \dot{y}_h$ (3.45)

It should be noted that in a conservative system the energy due to vertical velocity plus potential energy, which includes positional energy and energy stored by the spring, is constant. Therefore 1., seen as ground reaction force, contains information on the mass acceleration as well. Given this analogy, a further strategy outputting unconstrained acceleration was developed.

Potential inputs for 1. are position, velocity or force/acceleration of the grip. Analysing 1., it is observed that the ground reaction force feedback causes the interface grip to move vertically if the user does nothing, while the user has to hold on the grip, applying an equal and opposite force to the feedback, to maintain the grip in a still position. Drawing an analogy to human biomechanics, a runner has to apply force in their muscle at each contact phase for the sole purpose of not 'stumbling' onto the floor, while they have to apply a greater amount of force if they want to accelerate. Therefore, holding the grip in a still position was considered as applying no extra force, while a movement along or against the force would result in a negative or positive input.

Given a point mass landing on a movable surface, the total acceleration of the mass is given by:

$$m\ddot{y} = F_{appl} - F_{react} = F_{in} \qquad (3.46)$$

where F_{appl} is the total external force applied to determine the surface kinematics, F_{react} is the force needed to maintain the surface at its original height and F_{in} is the extra force applied on top of F_{react} to change the acceleration of the surface and system; reference positive direction pointing upward. The acceleration of the mass and surface are coupled while in contact and decoupled after take-off. Therefore, a mechanically meaningful input to the system would be $F_{in} \propto \ddot{y}$.

Preliminary tests showed that the user finds controlling force through acceleration challenging as a movement in one direction (say positive) could still result in a force in the opposite direction (as, say, a velocity in the positive direction which decreases in time would output a negative force); given the small room of operation of the haptic interface, avoiding deceleration was found to be nearly impossible (as the user would reach the physical limits of the grip area of movement). Therefore, velocity and position were tried as inputs. Velocity is commonly used as haptic input for admittance devices, and solves the problem of unintuitive negative force when moving the in positive direction, but can still resolve in the user reaching the physical limits of the interface. Position input is the standard more direct form of control.

3.4.2 Adjusting variables

While equations for the possible couplings were provided in the previous section, no information was yet given of possible different implementations of these. Several variables had to be decided when implementing the couplings:

1. Direction of positivity vs. negativity: choosing whether moving upwards apply a positive or negative force / an increase or decrease in stiffness.
2. Span of applicability of the input: choosing in which phases of locomotion will the input have an effect on the system. For force, no input can be applied during flight, and it is left to decide whether the input should be applicable during the whole contact phase or parts of it. For stiffness, input could possibly be applied during contact phase and during the second part of flight phase (after the apex is reached), in which case the angle of attack is indirectly modified.
3. Possible haptic feedback change to indicate if the system can receive input: in couplings where the feedback consists of a constrained position/movement of the grip, the virtual spring stiffness (and dumping value when applicable) causing the constraint could be soften, when input is receivable, to encourage the user to shift the grip from this zero-input position.
4. Choice of parameters. For the input, the map certain position/velocity/acceleration values of the grip onto a certain value of force/stiffness input to the system had to be decided. Similarly, the output

quantities had to be scaled to an output force appropriate for a user to feel its action but not interfere too much with their input action.

As mentioned above, preliminary tests were carried out to choose among the possible couplings. For each coupling, the four factors explained above were optimised independently, while keeping the other factors constant. Cross testing was found unnecessary as the choice of 1., 2., and 3. appeared obvious from the tests and the choice of 4. (pre-filtered), being continuous, did not affect the results by a great amount; it is anyway not likely that the choice of 1 parameter could affect the others.

4 Implementation and data analysis

4.1 Implementation of the testing system

The testing system consists of the locomotion model, visual and haptic feedback, and haptic input from the user, as explained in Section 3. An overview of the implementation blocks that form this system is shown in Figure 4.1. The program is divided into two main loops which run independently, but yet communicate with each other: the visual feedback + locomotion model loop (blue), and the haptic coupling loop (green). The former block is responsible for progressing the kinematics of the system, checking their status with respect to the target of the trial (whether successful, crashed or timed out), and displaying the visual feedback. The latter block is responsible for the haptic interaction with the user: outputting force and reading in the input to the system. Haptic output is related to system characteristics and is therefore calculated in the model block and passed to the haptic block, vice versa the input read by the haptic block is continuously passed to the model block to affect its kinematics. (*) indicates the equations of motion of the target system depend on the trial goal selected (Section 3.2), which consists of a model analogous to the user-controlled model for complex tasks, and simply of a constant velocity system for all major testing in this project.

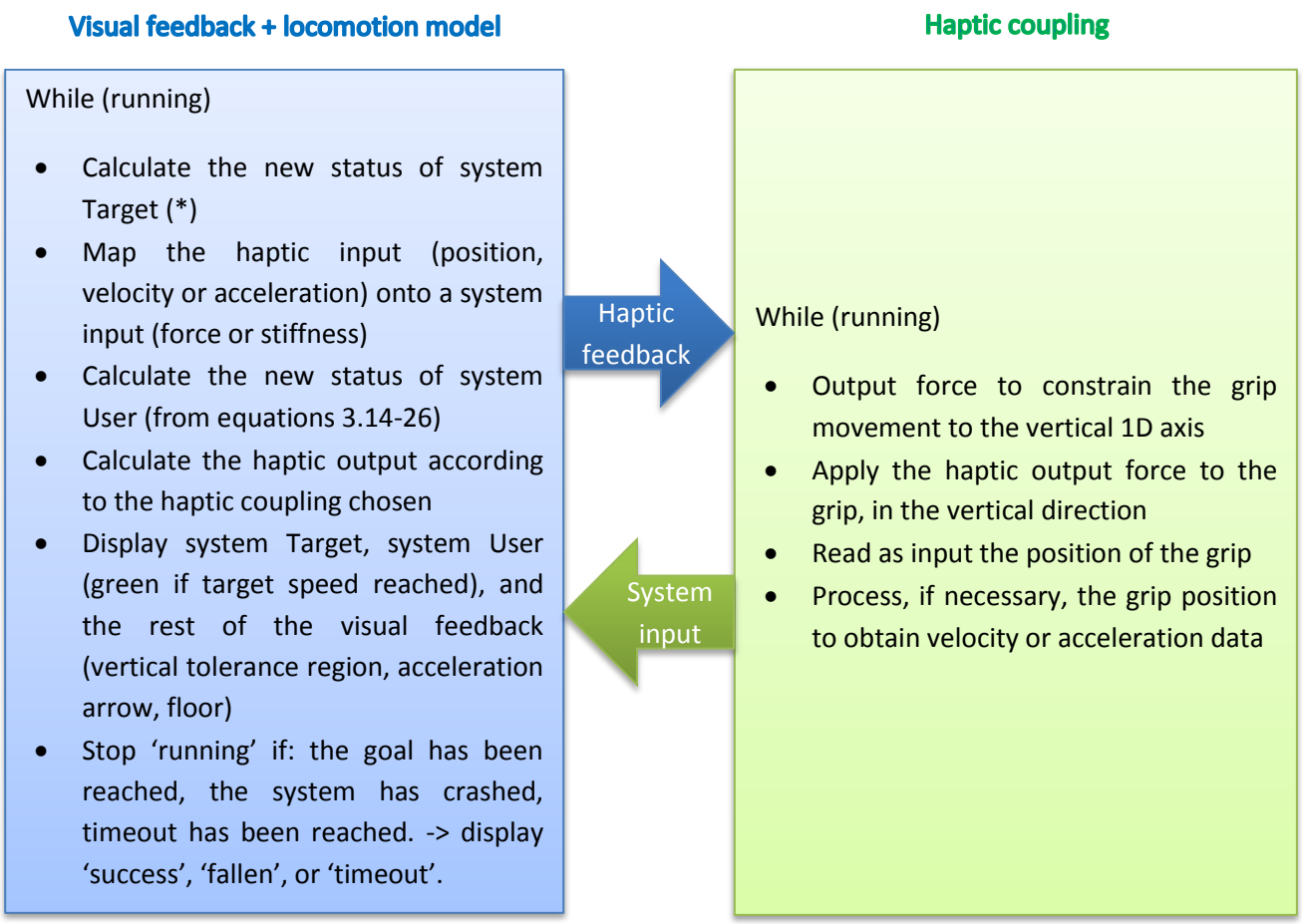

Figure 4.1: overview of main blocks of implementation which make up the system for testing. System User is the locomotion controlled by the user; (*) indicates the target system evolves according to the choice of target for the trials.

The program was implemented in C++ and made large use of OpenGL for the visual feedback. For implementing the haptic coupling, the sample program provided by Novint was used (a link in provided in **Appendix A**). The Visual Studio 2012 environment was used. The following sections analysed peculiar sections on the implementation.

4.1.1 Transforming the input and output of the haptic interface

The haptic interface which will be used in testing is the Novint Falcon (novint.com), an impedance device with 3 degrees of freedom, where the output to the user is in terms of 3D force, and the 3D position of the grip is read as input. In the Section, haptic couplings with different inputs and outputs have been discussed; this section will illustrate the strategies used to achieve this.

In **Section 3.4**, the strategy of outputting a constrained position or movement of the grip was used several times. This constrain is achieved by the mean two virtual springs whose rest position lead to the target grip position. This strategy is commonly called 'position error'. The output force is therefore F=0 when the grip is in the desired position, and

$$|F| = kd \qquad (4.1)$$

(pointing towards the desired grip position) when the grip is at a distance d from that position (using virtual springs of stiffness k). In particular, the 2 horizontal degrees of freedom where constrained for all tests to the zero position. Outputting a movement of the grip is achieved by changing the F=0 position of the grip in time. This strategy easily adapts to constraining the movement to a region and not interfering within this; this is achieved by calculating setting F=0 if within the region, and using **eq. 4.1** otherwise, with d=distance from the closest border of the region. When adopting the constraint feedback strategy, it should be noted that the input, yet in terms of position, is an indicator of the amount of force the user is applying.

Velocity and acceleration data can be easily extracted by taking the first and second derivative of the raw input data of position. Numerical approximations of the derivatives were used:

$$\dot{y}(t) \approx \frac{y(t)-y(t-h)}{h} \qquad (4.2)$$

$$\ddot{y}(t) \approx \frac{y(t)-2\,y(t-h)+y(t-2h)}{h^2} \qquad (4.3)$$

where $y(t), \dot{y}(t), \ddot{y}(t)$ are the vertical position, velocity and acceleration of the grip at time t, h is some time delay, and time instant t-h is previous to time instant t.

A moving average filter was used to smooth velocity and acceleration data. The final formulas used are:

$$\dot{y}(t) \propto \sum_{n=0}^{99} y(t+nh) - \sum_{n=0}^{99} y(t+(n+100)h) \qquad (4.4)$$

$$\ddot{y}(t) \propto \sum_{n=0}^{99} y(t+nh) - 2\sum_{n=0}^{99} y(t+(n+100)h) + \sum_{n=0}^{99} y(t+(n+200)h) \qquad (4.5)$$

where $\propto$ indicates the proportionality, and h is the time of one program iteration (2-3ms, approximately constant when averaged over 100 iterations). As the velocity and acceleration were arbitrarily scaled to values optimal in terms of feedback sensation, the denominator term was not calculated.

4.1.2 Model derivative and Standardised time step

The equations of motion (**3.14-26**) were implemented using the numerical approximation of **equation 4.2**. The program iteration changes between 2 to 3ms, which can mean a change of 50% its value. Therefore, fixing the time step h of the approximation would result in unrealistic display of the model behaviour in time. To this extent, the library Chrono (msdn.microsoft.com) was used to time each iteration of the program and evolve the model in a real time frame. Calling t_{it}(n) and h(n) the time of iteration n and the chosen time step for that iteration, achieving realism would imply: $t_{it}(n) = h(n)$. Due to the complexity and instability of the model, h=2-3ms and the parameters discussed in **Section 3.1**, the model would diverge or crash within the minute. A constant h(n)=1μs was chosen, allowing the program to run for ca. 2 minutes before any change in periodic behaviour of the stable system could be noticed, and ca. 3 minutes before the system crashed. Time realism was achieved by looping over the equations of motion until the model had evolved for a total time equal to the real iteration time. As this would imply displaying the system on the screen moving at ≥5m/s, an arbitrary scaling factor was used to choose the display speed. The final loop implemented is (in pseudocode):

$$
\begin{aligned}
&while\ \left(h * n_{loopiter} * scaling_{dispSpeed} \ < \ t_{it}\right)\\
&-\ apply\ equations\ of\ motion\ to\ state\\
&-\ t_{it} = current\ time - end\ time\ of\ previous\ state\ display\\
&end\\
&save\ and\ display\ new\ state
\end{aligned}
$$

4.2 Classification of input strategies

As mentioned in **Section** Introduction, the goal of this project entails analysing strategies which subjects use to control and/or learn stable smooth locomotion. An overview of the results showed that nearly all input strategies could be classified into 5 very specific categories. Paradigms of input shapes for the categories are shown in **Figure 4.2**. A sixth broader category was added to include a variety of more complex input strategies. One input curve consists of the input during a one period of the system being receptive to it. As, for the haptic coupling analysed, the input force was controllable during the second part of contact phase (after the maximum contraction of the spring), each contact phase generated one input curve to analyse, at time starting from the moment of maximum compression of the spring until the moment of take-off. A strategy was considered in terms of the shapes of the force input vs. time (taken from the start of the input phase) curve.

An automatic classifier was developed to classify the inputs into the closest category. Classification operated on the gradient of the force input, approximated by **eq. 4.2** and filtered by a moving average filter averaging over 50 points. Features extracted from the gradient curve were: peaks, flats

The moving average algorithm gave overall good results in terms of extracting only important peaks and not irrelevant local changes, on top of this few algorithms to remove false positives were adopted, which mainly acted on merging neighbouring similar peaks and on removing nuisance at the start and end of the gradient curve.

A decision tree illustrating the approximate classifier is shown in Figure 4.3; the real classifier was more complex as it involved strategies to remove category-specific false positives. The depth-first search strategy was adopted to navigate through the tree, meaning if a branch of the tree led to a successful classification, no search happened through the other categories. All force input were scaled to have a maximum value of 1. The classifier was manually trained to fit most of the preliminary tests data and was used to classify data from the major tests. All inputs were then double-checked manually; the confusion matrix of the classifier is shown in Table 4.1. The accuracy is:

$$accuracy = \frac{number\ correctly\ classified}{total\ number\ samples} = \frac{822}{853} = 96\%$$

A link to the complete classifier code is found in Appendix A.

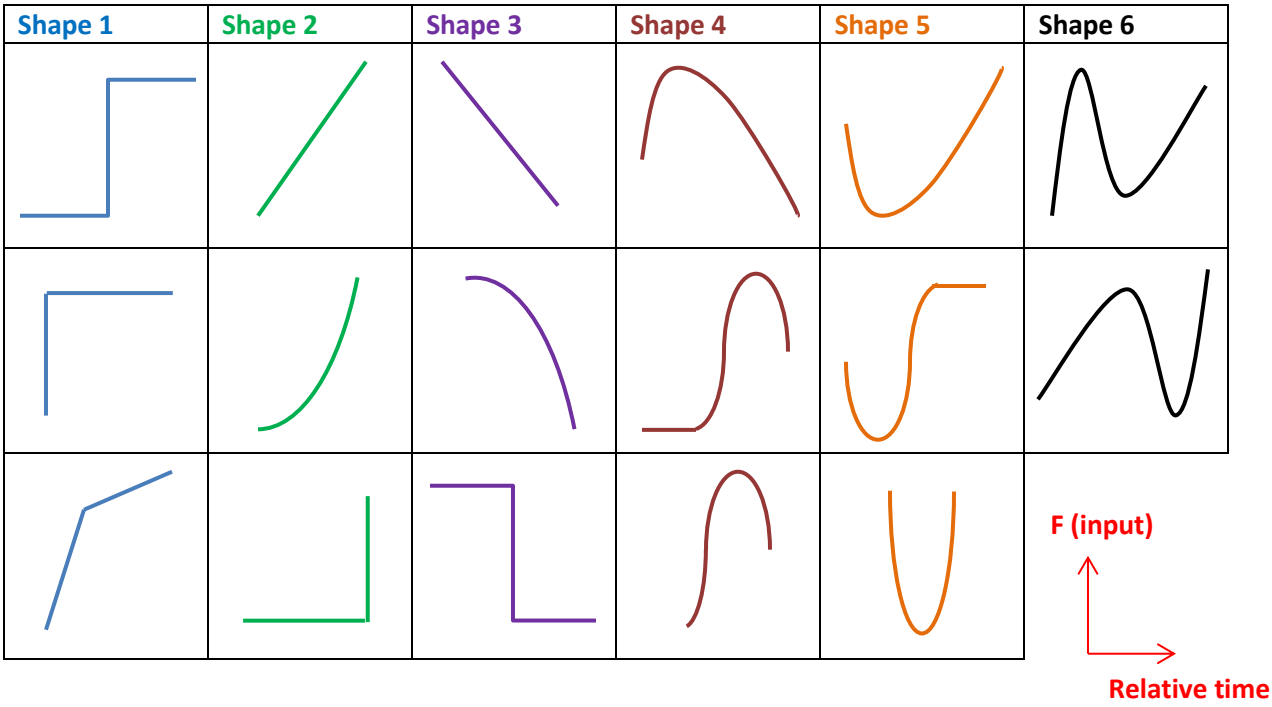

Figure4.2: some examples of curves which would belong to the category indicated. For each of the curve, the x-axis represents time and the y-axis represents input force.

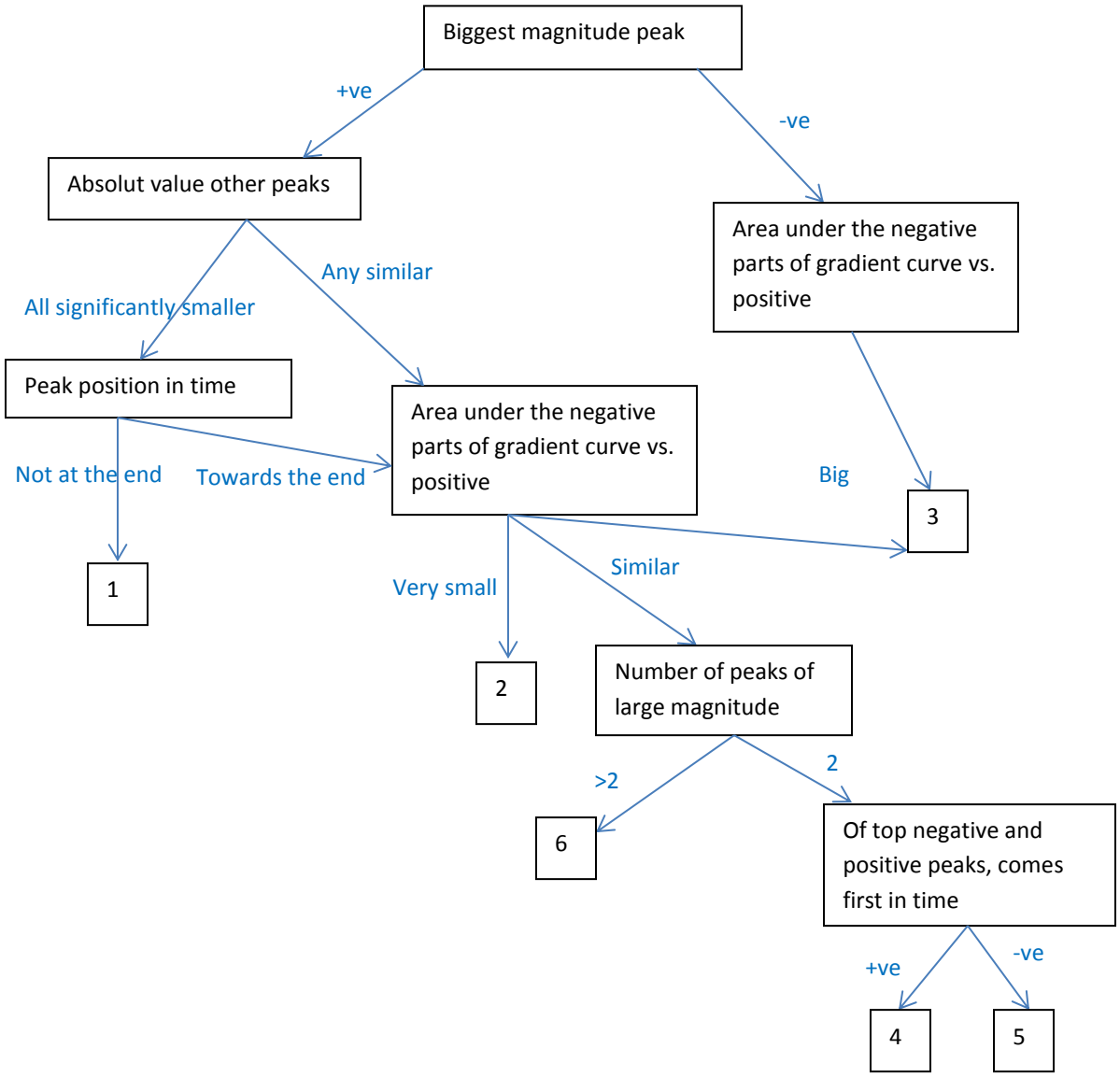

Figure4.3: approximate decision tree of the input category classifier. All features are relative to the gradient of the input force.

$actual$ \ $classified$	**1**	**2**	**3**	**4**	**5**	**6**	**None**
1	313	9	0	1	0	0	0
2	2	200	0	1	3	0	0
3	0	0	48	0	0	0	0
4	3	0	3	117	0	3	0
5	0	1	1	0	116	0	0
6	2	0	0	0	0	28	2

Table 4.1: classification matrix for the input strategy classifier. The matrix indicates the number of strategies belonging to category 'actual' that were classified under 'classified'.

5 Testing and results

5.1 Preliminary tests

Several possible haptic couplings were explored in **Section 3.4**. It was not feasible to carry out major experiments for more than 3 couplings due to time and test subject constraints. Therefore, preliminary tests were carried to select the 3 most stable coupling options for further testing.

Two subjects were selected to test several coupling options, undertaking 5 trials for each coupling. Testing conditions are explained in **Section 3.2.** The goal was to match a horizontal velocity of 7m/s. The subjects already had experience with the locomotion model and with the haptic control of it, as they had tried it during development. **Tables 5.1** and **5.2** summarise the tests taken and their outcome. The outcome is measured in terms of successful trials and average time of achievement of this (if the subject succeeded at least 3 trials). For details on what coupling the abbreviations stand for, the reader should refer to **Section 3.4**. The temporal separation coupling was discarded as it caused jerky movement of the grip. The only couplings which showed an obvious learning along the trials were the ones involving a region of tolerance, their overall performance was though inferior to other couplings.

---

positive verse	feedback	Haptic output gain	range/ gain	Other	subj 1: n success	subj 2: n success	subj 1: mean time	subj 1: mean time
Down.	Pos. error, single pt.	5	0 to 60kN/m	-	0	0	/	/
Up.	Pos. error, single pt.	5	0 to 60kN/m	-	5	0	50s	/
Up.	Pos. error, single pt.	10	5 to 50kN/m	-	5	3	27s	52s
Down.	Pos. error, single pt.	10	5 to 50kN/m	-	4	1	81s	/
Up.	Pos. error, single pt.	10	5 to 50kN/m	High feedb. When k not adj.	5	2	48s	/
Up.	Pos. error, toler. area	10	5 to 50kN/m	-	5	3	34s	62s
Up.	Pos. error, toler. area	10	5 to 50kN/m	Adj. only in contact	0	0	/	/
Up.	Pos. error, single pt.	10	X100	Incremental change	1	1	/	/
Up.	Prop. to position, toler. area	10	5 to 50kN/m	Error augmentation	5	0	64s	/
Up.	constant, toler. area	10	5 to 50kN/m	Error augmentation	0	0	/	/

Table 5.1: tests for stiffness input. Columns indicate the status of the most changed parameters. When not indicated in the column 'other', the following is assumed: position, linear (vs. incremental) input adjustable during contact and downward flight, guidance (vs. disturbance) output feedback, same output feedback whether k adjustable or not. Average timings of success (right columns) are calculated when the subject succeeded at least 3 trials. The best performance is highlighted.

positive verse	feedback	When adj	Feedback when not adj.	Haptic output gain	Input	subj 1: n success	subj 2: n success	subj 1: mean time	subj 1: mean time
Up.	Pos. error, mass mov.	Contact	Same	10	Pos.	5	3	37s	45s
Down.	Pos. error, mass mov.	Contact	Same	10	Pos.	5	4	37s	47s
Down.	Pos. error, mass mov.	Upward contact	Same	10	Pos.	4	5	50s	44s
Down.	Pos. error, mass mov.	Downward contact	stiffer	10-30	Pos.	3	2	91s	/
Down.	Pos. error, mass mov.	Upward contact	stiffer	10-30	Pos.	5	5	48s	61s
Down.	Ground react.	Upward contact	same	1/2000	Vel.	5	5	66s	51s
Up.	Ground react.	Upward contact	same	1/2000	Vel.	4	5	46s	81s
Down.	Ground react.	Upward contact	same	1/2000	Acc.	0	0	/	/
Down.	Ground react.	Upward contact	same	1/2000	Pos.	5	5	41s	50s

Table 5.2: tests for force input. Columns indicate the status of the most changed parameters. When not indicated in the column 'other', the following is assumed: linear (vs. incremental) input, guidance (vs. disturbance) output feedback, input range=-5 to 5 kN. Average timings of success (right columns) are calculated when the subject succeeded at least 3 trials. The best performances are highlighted.

In analysing the performance, the most important measure was stability, and secondly the speed of achievement of the task. Selecting the best strategies for stiffness, force-position error, and force-ground reaction, the following 3 coupling were selected for further testing:

1. Stiffness input (linear, from position), adjustable during contact and downward flight, positive in the upward direction. Position error (guidance) output feedback to a single stable point, same output feedback whether k adjustable or not. Output haptic gain=10, input stiffness range 5 to 50kN/m.
2. Force input (linear, from position), adjustable during upward contact phase, positive in the downward direction, stiffer output when F not adjustable. Position error feedback guiding the grip to the mass vertical position. Haptic output stiffness: 10, 30. Input range -5 to 5kN.
3. Force input (linear, from position), adjustable during upward contact phase, positive in the downward direction, same output when F not adjustable. Ground reaction force feedback. Haptic output gain: 1/2000. Input range -5 to 5kN.

These couplings are highlighted in **Table 5.1 and 2**.

5.2 Principal tests

5.2.1 Testing methods

The system used for the testing is discussed in **Section 3.** The target flight horizontal velocity was set to be constant, equal to 7m/s. The testing was performed using the 3 coupling methods which resulted successful in

the preliminary results (**Section 5.1**). Nine subjects undertook 10 trials plus a familiarisation trial for each of the 3 haptic couplings, for a total of 33 trials each.

Another 5 subjects took part in some of the trials but their data had to be discarded. 2 of these subjects, who had previous virtual haptic experience, were found too distracted as they were performing another activity while testing the system. One subject, with no previous haptic experience, refused to finish the tests as they could not stabilise the system. The other 2 subjects, who had no haptic experience, could not achieve modifying the system kinematics and applied harsh force on the haptic interface so they were not asked to perform the rest of the tests.

Of the nine which completed the experiments, three had previous experience with controlling the system with the interface (two of these were the subjects who took the preliminary tests). The other six subjects had previous experience with the haptic interface, and in particular they all had previously learnt to control, with the same interface, a monopod system jumping in the vertical direction[1].

Tests were organised so that each subject would take all 10 trials for a coupling option, wait for 2 hours to few days, then test the next coupling. The three experienced subjects, and the other six subjects, were evenly assigned to the tasks so that each of the 3 couplings would be tested as first by one experienced subject and two other subjects, and so on. These precautions are meant to limit the effect that learning one coupling would have on testing the next coupling.

Protocols were prepared for the subject to read before the testing of a new coupling method, a link to them is in Appendix A. The subjects were informed of:

- the system they were going to control (ie. running leg),
- the goal of matching a target speed (while staying within a region of tolerance)
- the kind of haptic and visual feedback they would receive,
- what they would input, how and when could they
- the conditions of falling, succeeding and timing out
- the structure of the overall test (1 familiarisation + 10 trials)

In addition, a hint on controlling the system was given, which stated (similarly in all protocols):

“ Apply positive force to accelerate. The main issue will be to accelerate in the horizontal direction rather than vertical. To do this, wait to apply force until the angle of the spring is flat enough. Apply negative force to decelerate, the angle at which you apply the force will determine which direction you decelerate . “

On the first of the ten trials, subjects were guided through auditory feedback in terms of when and how they should apply the input. The subjects were not informed of this feedback as otherwise it is expected their motor cortex would not make as much use of the learning experience (Marchal-Crespo and Reinkensmeyer, 2009; Sigrist et al., 2012; Powell and O’Malley, 2011). These forms of extra help were adopted after the failure of several subjects to control the system, as test subjects and their available time were limited. For all (but familiarisation) trials, the state of the system ($x, \dot{x}, y, \dot{y}, z_{ground}, \dot{z}_{ground}$), the value of the input, and the time stamp, at which these were taken, were recorded and are analysed in the next section.

[1] Subjects had performed tests for another student who implemented a vertical motion SLIP system.

5.2.2 Performance and learning results

In this section, results from the principal tests in terms of subjects' performance, and evolution of this along the 10 trials, are presented.

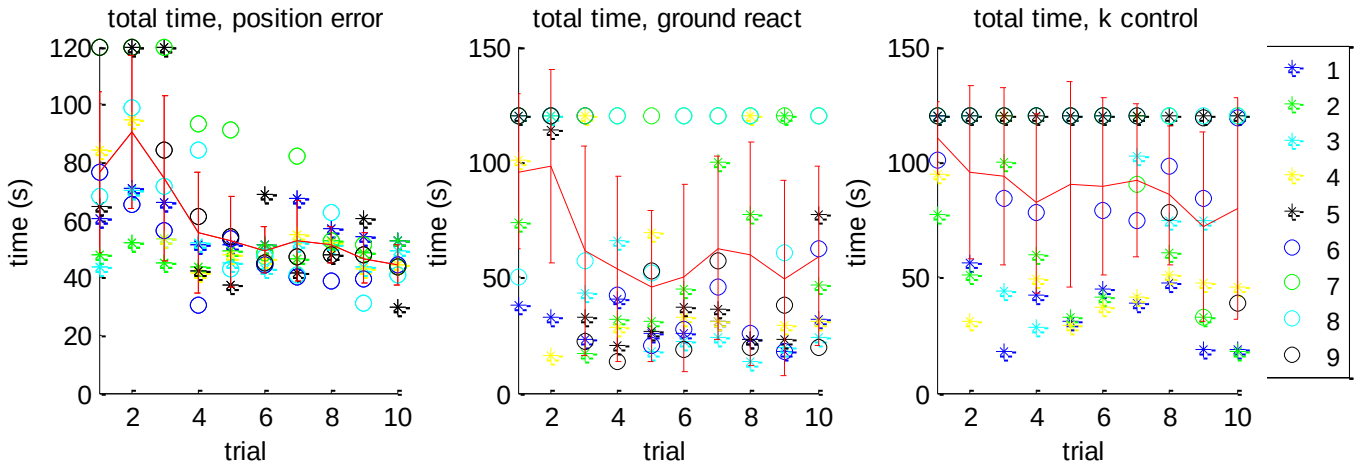

Figure 5.1: total time taken by the subjects to succeed the trial, evolution during trials, for the 3 haptic couplings used. Individual data is stemmed as 'o' or '*', the red line represents the mean and standard deviation across subjects. Unsuccessful trials times are set to 2mins (as timeout).

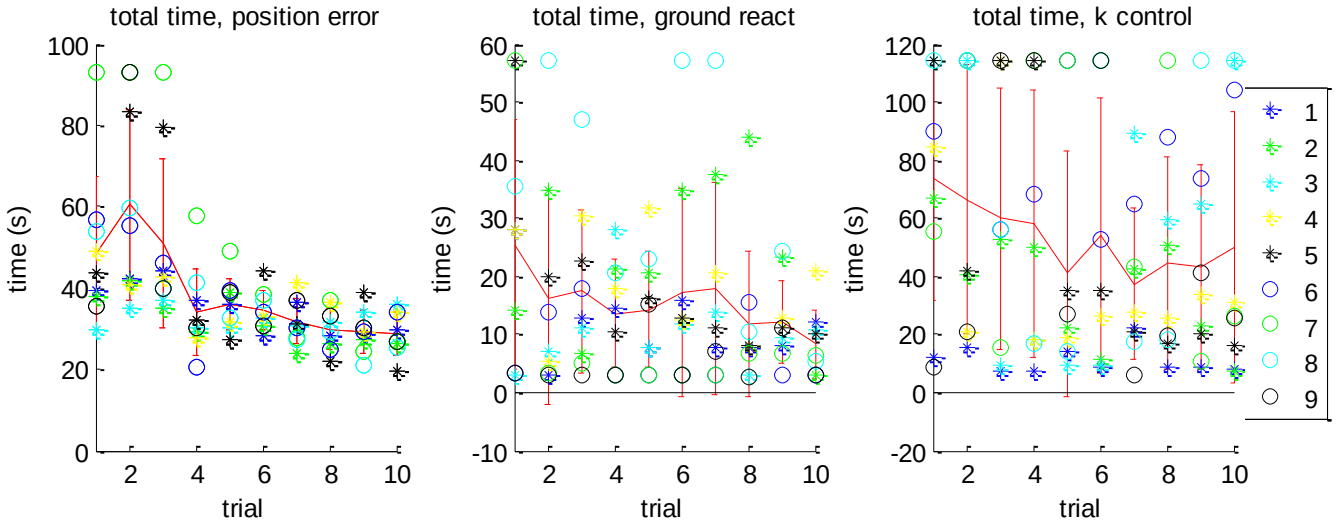

Figure 5.2: total time taken by the subjects to reach the velocity 6.7 m/s for the first time, evolution during trials, for the 3 haptic couplings used. Individual data is stemmed as 'o' or '*', the red line represents the mean and standard deviation across subjects. If the velocity was not reached, trials times are set to the maximum successful trial time across all data plus 10s.

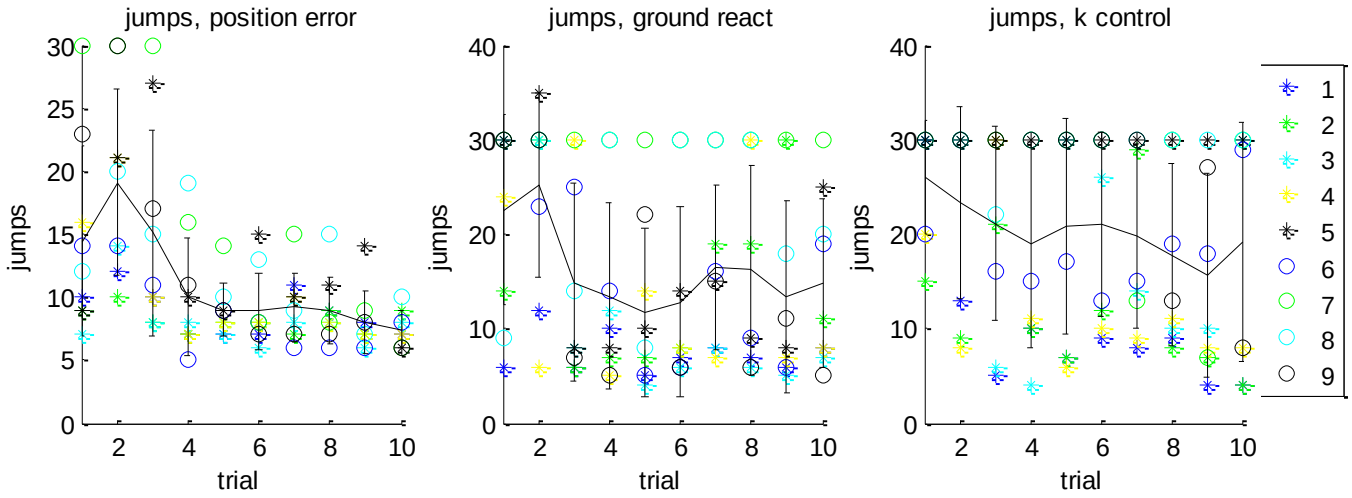

Figure 5.3: total number of jumps taken by the subjects to succeed the trial, evolution during trials, for the 3 haptic couplings used. Individual data is stemmed as 'o' or '*', the black line represents the mean and standard deviation across subjects. Unsuccessful trials times are set to 30 jumps.

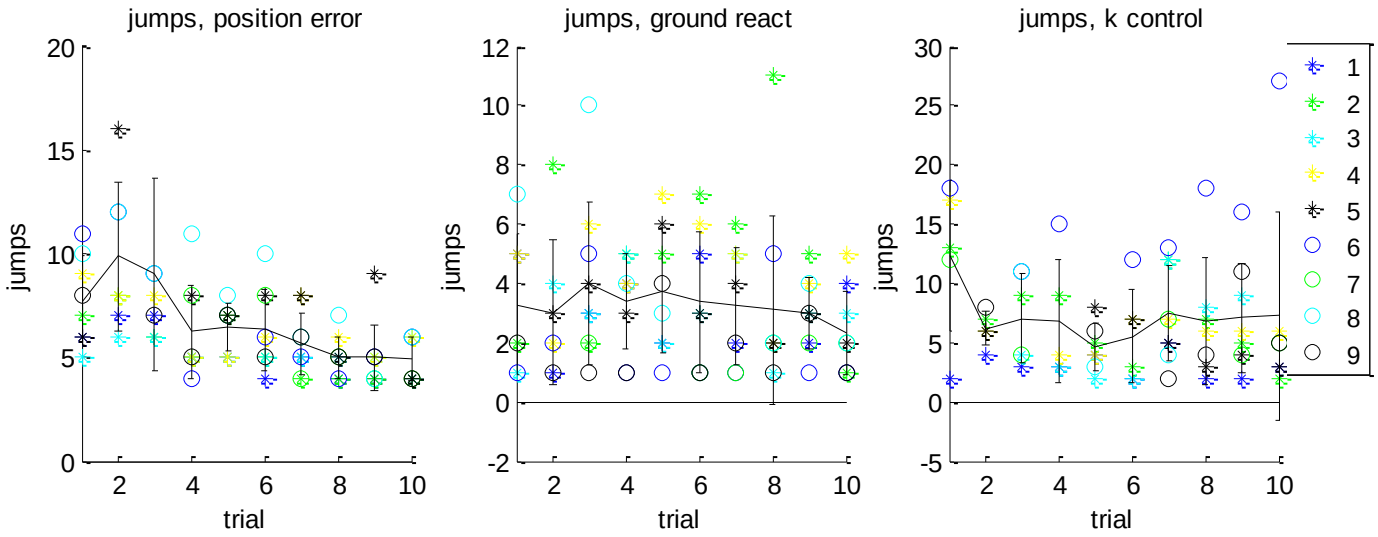

Figure 5.4: total number of jumps taken by the subjects to reach the velocity 6.7 m/s for the first time, evolution during trials, for the 3 haptic couplings used. Individual data is stemmed as 'o' or '*', the black line represents the mean and standard deviation across subjects. If the velocity was not reached, trials times are set to 15 jumps.

Figures 5.1 to 5.4 present performance measure for all users per each trial and coupling, and the mean and standard deviation across users, in terms of:

1. Total time to succeed the trial, measured in seconds. This measures directly what the subjects were told to achieve during the trial.
2. Total time taken by the subjects to reach for the first time horizontal velocity in flight phase of 6.7m/s. This value corresponds to the lower boundary of the target velocity tolerance. As subjects found more difficult to decelerate (if they happened to overshoot the target speed) than accelerate by a noticeable amount, it is possible that this measure of performance shows learning better than 1.
3. Total number of jumps taken to succeed the trial. As subjects can only control the input to the system during (a certain part of) contact phase, and that every jump offers similar possibility of accelerating (meaning, a longer contact time does not necessarily imply more room for improvement), counting jumps might offer a better performance measure than time.
4. Number of jumps to reach horizontal flight velocity 6.7m/s for the first time.

5.2.3 Input strategies adopted

As will be discussed in **Section 6.1**, the only haptic coupling that can be considered successful is the one involving position error feedback to guide the grip the position of the system mass. This section analyses the different curves of input in time that the 9 subjects used in order to achieve the goal using this specific coupling. This section analyses the different curves of input in time that the 9 subjects used in order to achieve the goal. 6 categories of input are identified, on which the input data are classified. The reader should refer to **section 4.2** and **figure 4.2** for an overview of the category curves, as well as classification methods. Statistics on the use and performance of these strategies are reported in this section.

Figures 5.5 to 11 show respectively:

5. How often does each subject adopt a certain strategy respect to the other ones, measure taken over all trials
6. How much change in horizontal velocity of flight (in m/s) from one jump to the next does each strategy achieve on average. Data are differentiated according to the intention of the user to accelerate vs. decelerate (obtained by the error from the target trajectory)
7. Overview of the evolution of the applied input for each subject. For each user, mean data from the first 5 trials is compared to the second 5 trials. Data of the proportion of use of a strategy vs. the other ones, and of the improvement in acceleration of using certain strategies, is taken. The difference of these two measures between the first and second half of the trials is taken. The absolute differences are scaled by the maximum differences of that measure across all trials. Therefore, the figure indicates both how much does a subject change their technique compared to other, and the means of this change. Only inputs to the purpose of accelerating are considered.
8. Evolution of performance (gain in velocity) across trials, averaged across subjects, for each strategy category.
9. Evolution of use (proportion) of a strategy across trials, averaged across subjects.
10. Similarly to 7., this figure shows the evolution in performance by averaging across the first 5 and the second 5 trials. Data are shown per user per strategy category.

11. Similarly to 7., this figure shows the evolution in use of a strategy by averaging across the first 5 and the second 5 trials. Data are shown per user per strategy category.

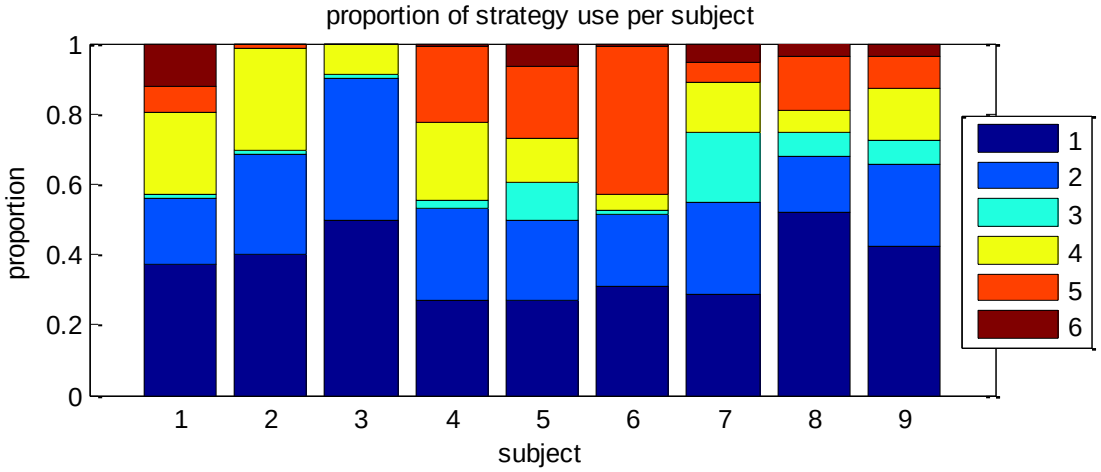

Figure 5.5: proportion in which each strategy is used, per subject (along all trials).

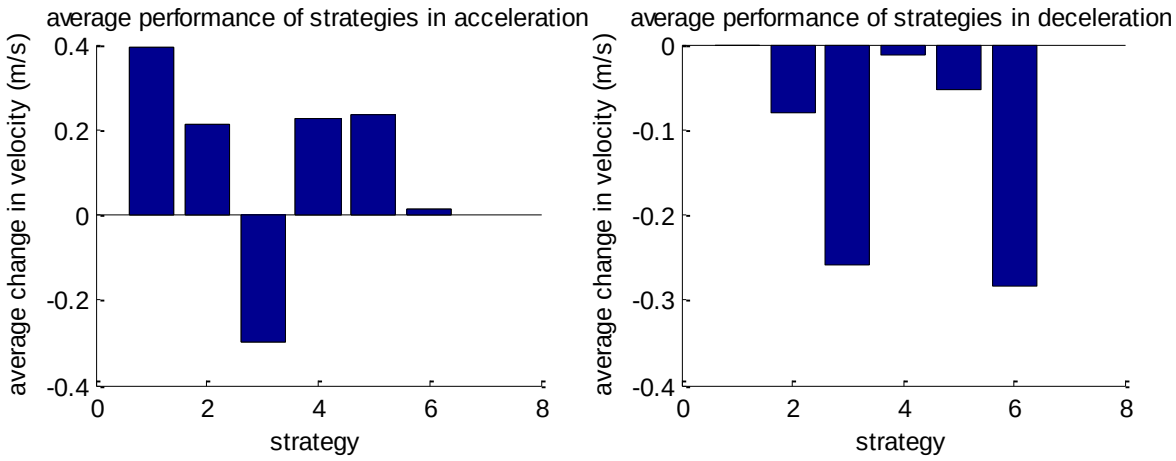

Figure 5.6: average change in flight horizontal velocity achieved, from one flight phase to the next, given the use of a certain strategy and user intention. The intention is deduced by considering whether the previous velocity was above or below the target level.

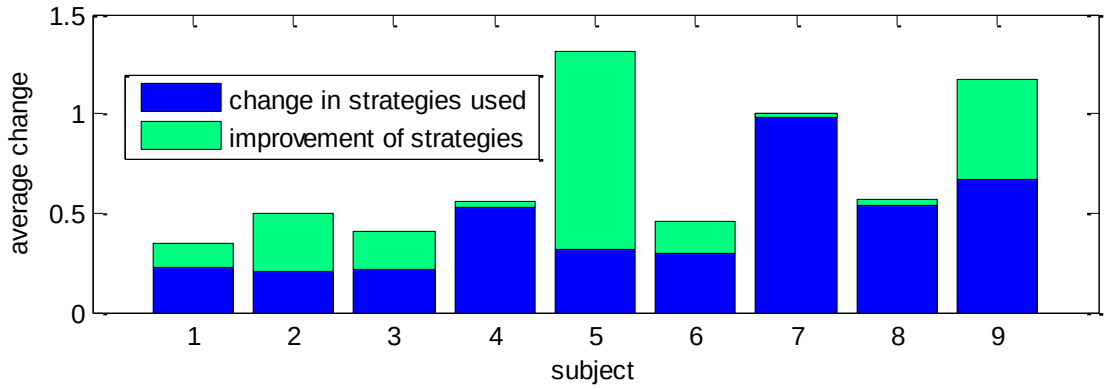

Figure 5.7: overview of the change in technique of control undertaken by each subject along the 10 trials. To notice change, the first 5 trials are compared to the second 5 trials. Changes are either in using different category of strategies, or in improving the performance of the used strategies. The total amount of change is scaled by the maximum change per type across all subjects. The graphs indicated therefore how much each subject changed compared to the other, and in which ways.

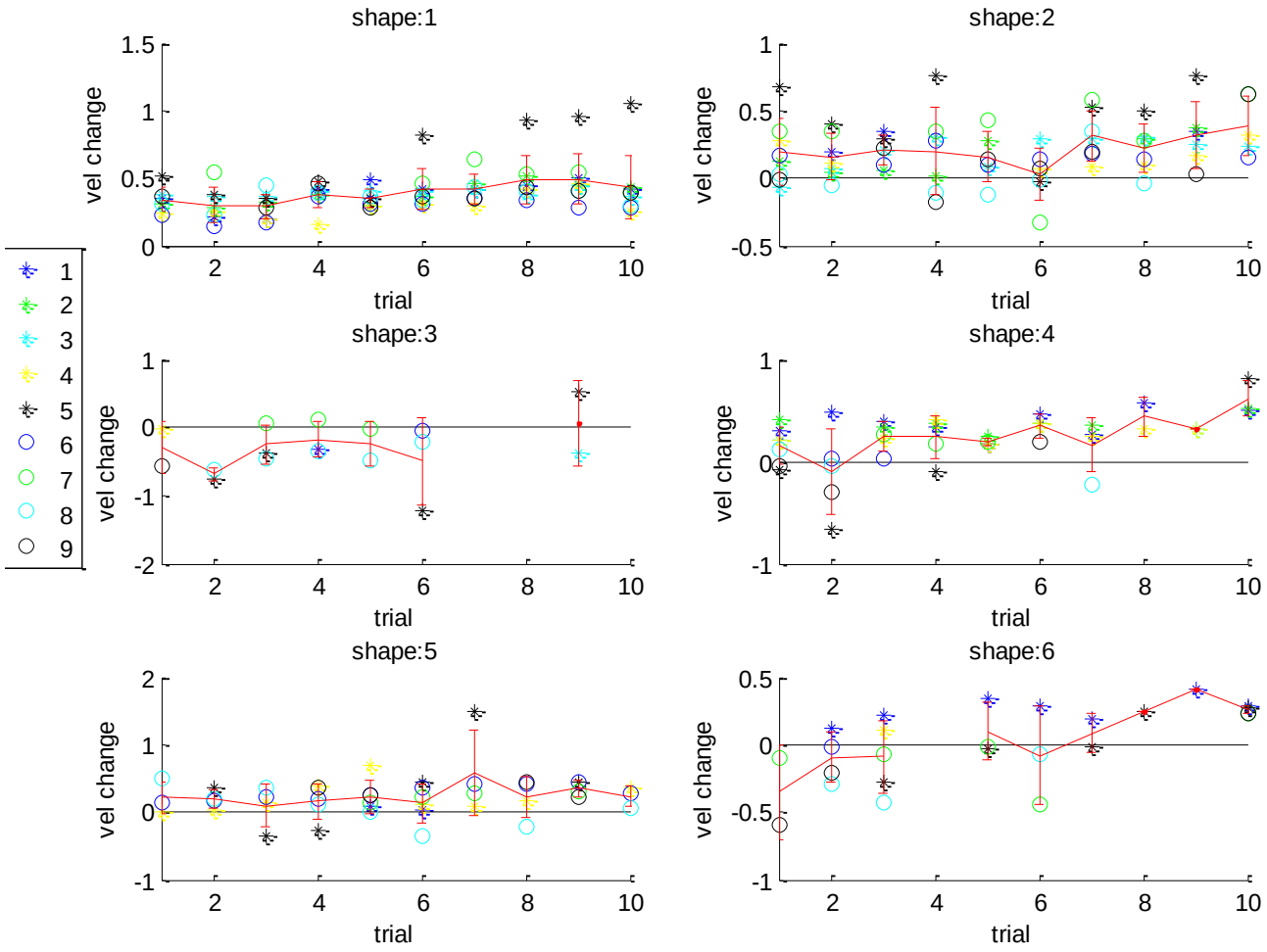

Figure 5.8: change in flight horizontal velocity achieved by each strategy and subject in each trial, and its evolution. The red line represents the mean and standard deviation between subjects.

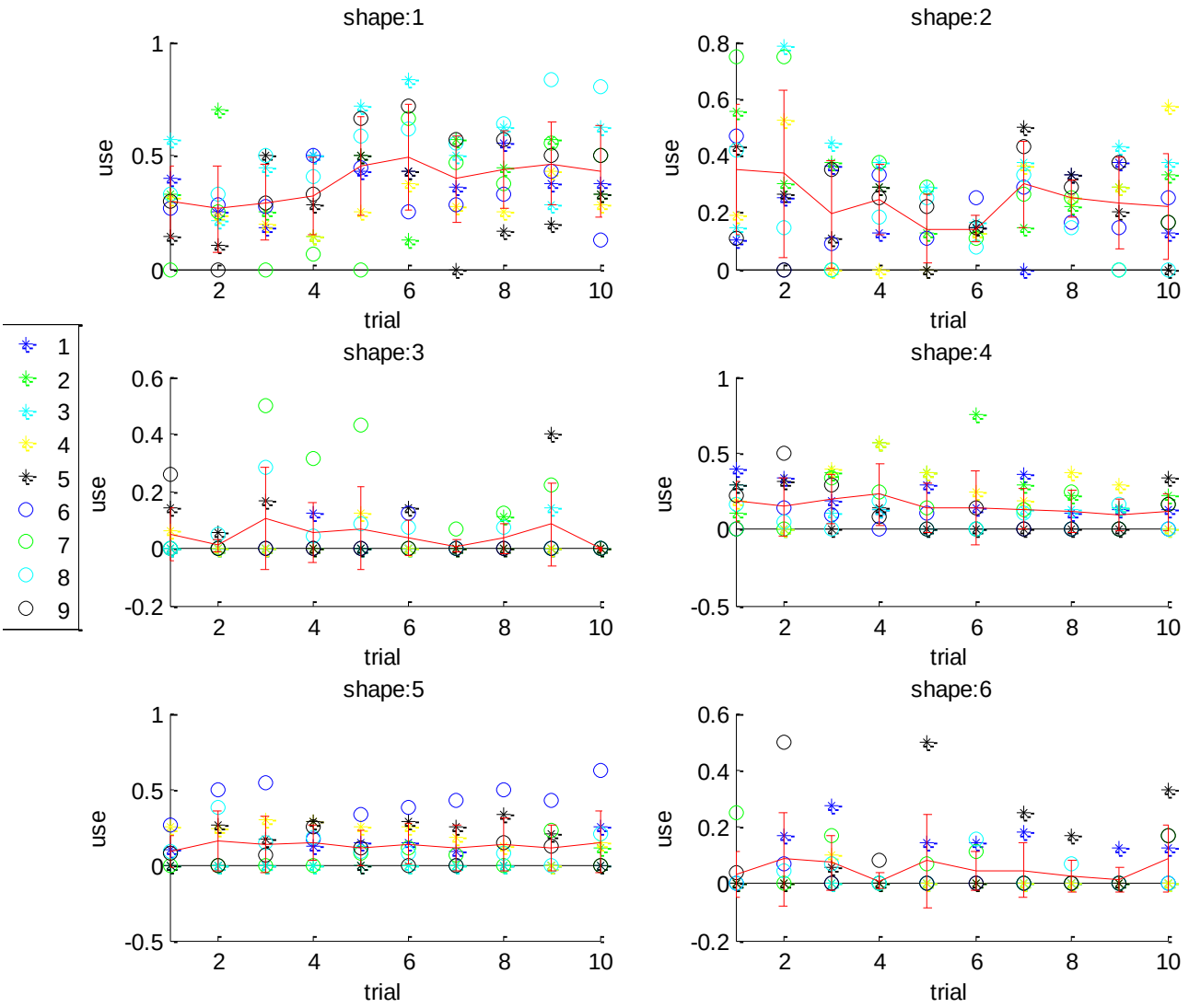

Figure 5.9: change in the use amount (as a proportion) of each strategy by all subjects in each trial, and its evolution. The red line represents the mean and standard deviation between subjects.

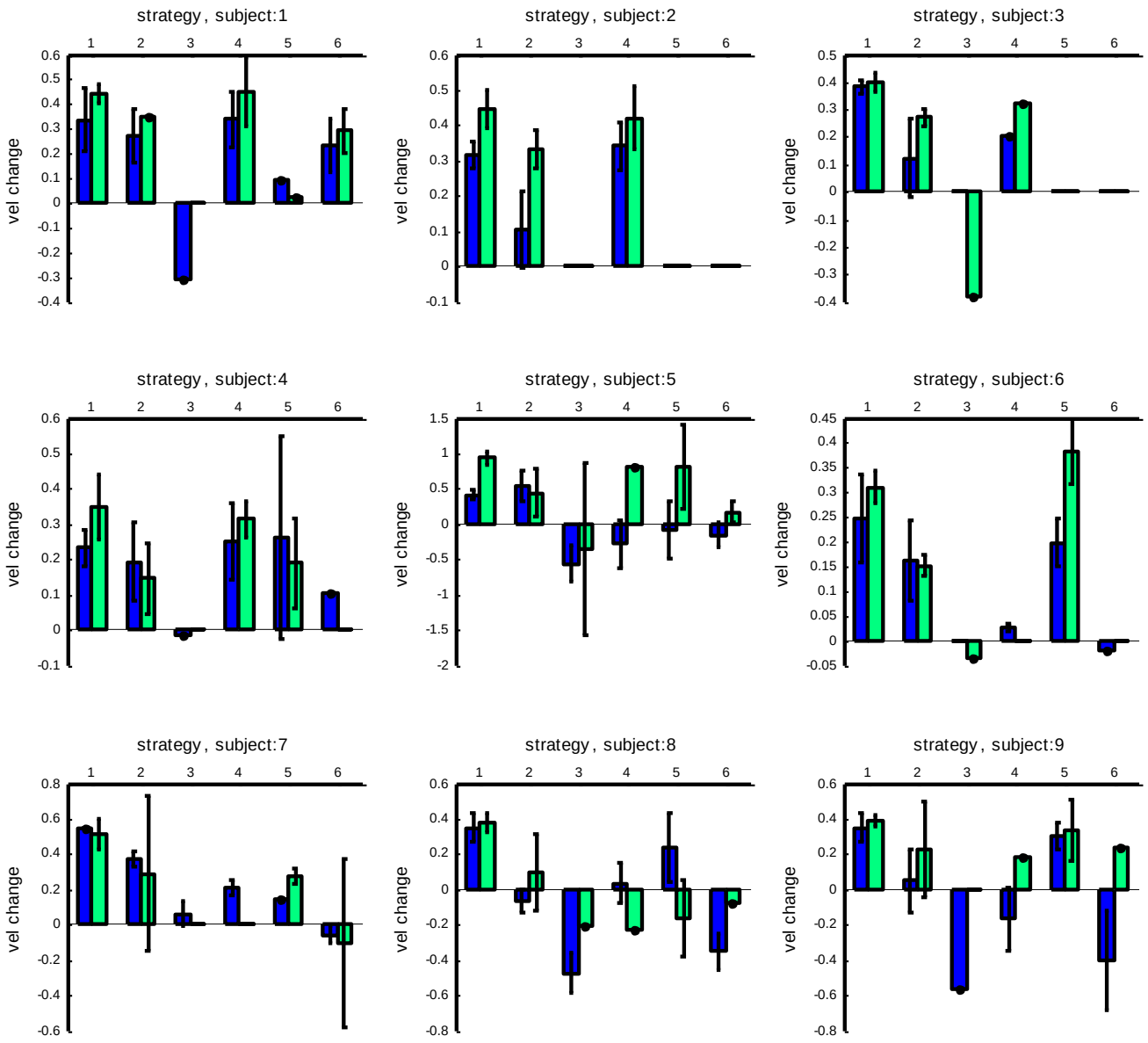

Figure 5.10: change in the performance of each strategy by all subjects. The evolution is shown by taking the average performance in the first 5 trials (blue) vs the second 5 trial (green).

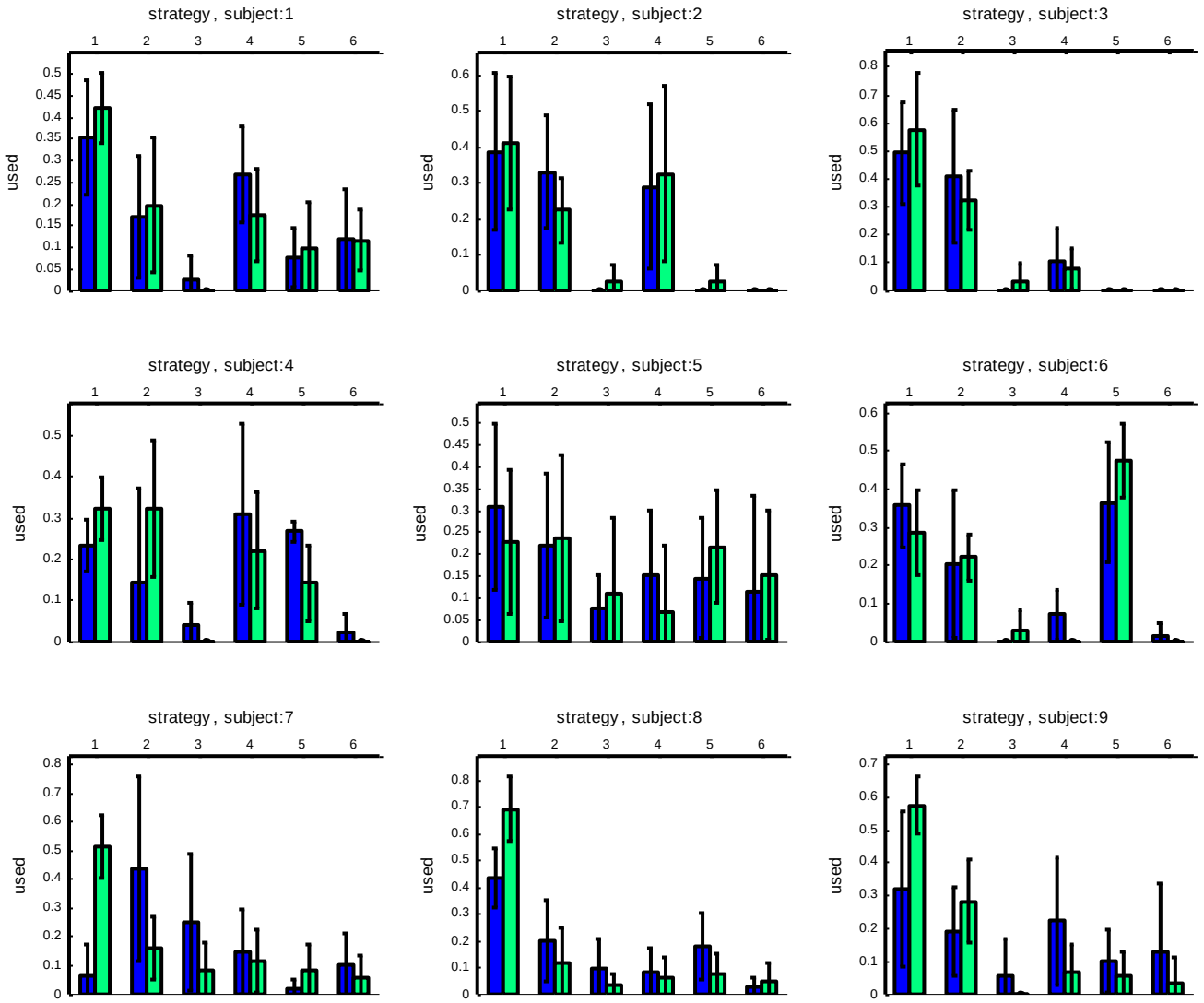

Figure 5.11: change in amount of use of each strategy by all subjects. The evolution is shown by taking the average use (as proportion) in the first 5 trials (blue) vs the second 5 trial (green).

6 Discussion

6.1 Performance of the haptic couplings

Figures 5.1 to 5.4 provide information on the performance and learning curve of the subjects when performing a test using a certain haptic coupling option. It appears clear from all four measures of performance that position error coupling option (outputting to the grip guidance to follow the system mass movement, and reading linear force as input) is successful, as no user fails the task after the third trial. Furthermore, a clear learning curve can be observed in the plots: in all four figures, the mean of trial 10 is significantly lower than the mean of trial 2[2], and the standard deviation bars do not overlap.

On the other hand, the couplings involving ground reaction force and stiffness control showed very poor performance, and no clear learning curve. In testing having ground reaction force feedback, 4 out of 8 subjects failed one or more tests of the last 3, and each of the 10 trials was failed by at least 1 trial. Even though some degree of performance improvement can be seen, the standard deviation bars of any trial overlap with the bars of all other trials, for all 4 measures of performance. Surprisingly tough, measures of success are discouraging, the mean time and jumps taken to accelerate to 6.7m/s are obviously lower than for the position error strategy in all trials. As the standard deviation of these values is really high, it is hazardous to interpret the meaning of this datum. Possibly, the ground reaction force sensation helps the subject to control locomotion, but the way the haptic interface delivers it (the subject has to apply force to stop the grip to applying a negative force) might cause instability. On the other hand, it is also possible that the negative force applied at the beginning of the input curve due to the haptic feedback (assuming most times it is challenging to completely oppose to this force) might help the system accelerating.

The coupling strategy controlling stiffness had the worst performance out of the three tests. For all trials, there were at least two subjects that could not reach the goal, and for 9 out of 10 trials there was at least 1 subject who could not reach a velocity of 6.7m/s. As for the ground reaction force, a slight performance improvement can be seen from the mean, but standard deviation bars are even bigger and more overlapping.

Therefore it can be concluded that the most successful strategy in controlling the system design is the position error feedback coupling.

6.2 Control strategies

The control strategies for the successful haptic coupling (position error) are investigated. Analysing the data, as in Section 5.2.3, 6 common strategies of movement, when inputting force, were found. The most successful strategy used for accelerating was 1. (Figure 5.6), which has the characteristic of presenting a very steep increase in force at one point in time before the system take-off, while keeping the force nearly stable at all other times (around 0 before the peak, and to some positive value after). As mentioned in Section 5.2, the key to achieving horizontal acceleration is to apply a positive force only at a proper time, directing the increase in energy to the wanted direction. Therefore it is not surprising that this peculiar input trajectory is successful. Strategy 1. is also the most used overall, and nearly most used by all subjects (2 subjects use strategy 1 and 2 nearly the same amount).

[2] The reader is reminded that trial 1 is biased, as the subjects received spoken guidance during this

The second most used strategy is 2., which consists of applying increasing force only at the end of the contact. Surprisingly, the performance of 2. is significantly lower than 1. The reason for this could be independent of the strategy itself but dependent on the situation in which the subjects most likely use the technique. In fact, strategy 1 degenerates into 2 if the time of contact is too short for the subject to apply the complete input curve they were aiming for (possible unconsciously). Therefore, a possible explanation of the worst performance of 2 compared to 1, is that strategy 2 in mostly adopted in contact phases harder to control. Strategies 4 and 5, which also entail applying a different force to different stages of the contact phase, have similar performance to 2.

While the performance of 3 and 6 in accelerating was really poor, the strategies were successfully used for deceleration. This seems obvious for strategy 3, where lower force is applied at the end of the contact phase. Strategy 6 is the most complicated, and as mentioned before subjects struggled to make the system decelerate if they happened to overshoot the speed. It is possible that subjects might have applied some semi-random movement resulting in 6 most times they could not decelerate. On the other hand, it is possible that more complex strategies are required for deceleration, and that some subjects manage to learn these.

6.3 Evolution of control

As mentioned in **Section 6.1**, a net curve of learning can be seen from the performance measure of the successful haptic coupling. The improvement in performance could be due to a change is strategy or to an improvement of the already used strategies of input. **Figure 5.7** presents a summary of the changes each user undertook to improve their performance. There is unanimous pattern: some subjects, such as 4, 7 and 8, largely changed the strategy they used, dropping rather than improving strategies which they found unsuccessful. Other subjects, mainly 5, maintained the strategies they first discovered but improved their performance more than any other subject. Overall all subjects present some degree of change in strategies used, while not all had improved previously used strategies in a noticeable manner. Among the users which least change their overall approach to the input, the 3 expert subjects (1 to 3) stand out, which is expected.

Looking at **Figure 5.9**, most curves of evolution of the use of a strategy along trials appear flat. The mean of strategy 1 increases noticeably but the standard deviation bars overlap by a large amount. In the same way, individual plots of **Figure 5.11** present a lot of variability. Considering **Figure 5.8,** the means of all strategies show an improvement of performance for acceleration purposes. While most standard deviations overlap, shape 4 and shape 6 show a meaningful increase in performance. For strategy 6, as mentioned for deceleration, this might indicate complex strategies can enhance performance if the subject learns them. It should be noted though that the final average performance of 6 was lower than strategy 1. Analyzing changes in performance for each user separately (**Figure 5.10**), a higher amount of significant results can be observed. For example, the improvement of strategy 1 is obvious for subjects 2 and 5, while it in inexistent for subject 7. On the contrary subject 7 improved strategy 5, which was not used by subject 2. It appears the subjects followed very different roots to learn the proposed system.

7 Conclusion

7.1 Evaluation of the project

In section 1, the goal of the project was defined in 2 stages:

3. Goal 1: to implement the system of Figure 1.1 successfully, in a way which would allow people to interact with the locomotion model
4. Goal 2: to investigate how do people control and learn to control locomotion, by finding possible patterns and/or key features.

As illustrated in Section 6, one haptic coupling was found which allowed all test subjects to be able to control the system; further a relevant curve of increase in performance was associated with the learning process of the subjects. The haptic coupling consisted of linear input force and position error feedback guiding the grip to follow the vertical movement of the mass of the model. The first goal of the project can therefore be considered a success.

As for all studies investigating the behavior of people, there is no discrete scale of evaluation for the success of goal 2. The fact that the learning curve, for the successful haptic coupling tests, was significant, suggests that the system implemented has the potential of emulating, to some degree of approximation, the real process of learning locomotion. Peculiar strategies of inputting the force, common across subjects, could be found. This can potentially indicate that features of learning locomotion can be extracted from the recorded data. On the other hand, it is totally possible the presence of these features in due to the setup of the system and haptic interface.

The development of a tactic to control the locomotion system was found to be very heterogeneous across different subjects. While it is feasible that people could adopt very different strategies when learning locomotion, it is likely that limitations in the experimental setup were the cause of variability. The data collected and analyze form a useful base for a future research in the field, as discussed in the following section. It cannot be concluded though that these data are relevant (nor the opposite).

7.2 Limitations of the project and suggested future work

The major limitation of the project was the lack of a pool of tests subjects willing to dedicate enough time to the experiment. This limitation affects the whole depth of the results obtained. For example, preliminary results had shown the haptic coupling involving control of stiffness could reach the goal velocity quicker than the coupling considered, by this report, successful; it is possible that with a proper amount of training, subjects would give better results using this coupling (which allows a more direct control of the leg dynamics). A bigger and less biased pool of tests subjects would also show whether the variability in learning is due to noise or it represents something meaningful. The first step for continuing the project would be therefore to collect better test data. Further testing should also analyze the system implemented for more realistic condition such as uneven and soft ground.

Improvements to the coupling, in particular visual, could make use of the fact that stimulating an outer point of view (guiding the subject to concentrate on the goal of their actions) improves the user's performance (see Section 2.2) A 3D view of the virtual environment, where the user sees as if they were inside this reality, could be used; but this requires a significant amount of training.

To extend this project to the analysis of a real exoskeleton system, testing should ultimately be carried out where the haptic interaction is with the lower limbs of the subject rather than with their upper limb. Finally, a more extensive data analysis on the input strategies could be carried out, for example comparing the angle of the leg to the amount of force inputted to the system.

References

By José L. Contreras-Vidal, Alessandro Presacco, Harshavardhan Agashe, and Andrew Paek, 2012. Restoration of whole body movement. IEEE PULSE

PETER GWYNNE 2012, Mobility machines, S16 | NATURE | VOL 503

Atilla Kilicarslan, Saurabh Prasad, Robert G. Grossman, and Jose L. Contreras-Vidal, 2013,High Accuracy Decoding of User Intentions Using EEG to Control a Lower-Body Exoskeleton, 35th Annual International Conference of the IEEE

Shiqian Wang, Wietse van Dijk , Herman van der Kooij , Spring Uses in Exoskeleton Actuation Design, 2011 IEEE International Conference on Rehabilitation Robotics

Federico Carpi, Danilo De Rossi , 2006, Non invasive Brain-Machine Interfaces

Reinhard Blickhan, 1989. The spring-mass model for running and hopping. Journal of Biomechanics 22, 1217–1227.

Andre Seyfarth, Hartmut Geyer, Michael Günther, Reinhard Blickhan, 2002. A movement criterion for running. Journal of Biomechanics 35, 649–655.

Daniel P. Ferris, Claire T. Farley, 1997. Interaction of leg stiffness and surface stiffness during human hopping. J. Appl. Physiol. 82(1): 15–22.

Daniel P. Ferris, Micky Louie, Claire T. Farley, 1998. Running in the real world: adjustments in leg stiffness for different locomotion surfaces. Proc. Roy. Soc. B. 265: 989–994.

Claire T. Farley, Han H. P. Houdijk, Ciska Van Strien, Micky Louie, 1998. Mechanism of leg stiffness adjustment for hopping on surfaces of different stiffnesses. J. Appl. Physiol. 85(3): 1044–1055.

Mojtaba Ahmadi, Hannah Michalska, Martin Buehler, 2007. Control and Stability Analysis of Limit Cycles in a Hopping Robot. IEEE transactions on robotics, vol. 23, no. 3.

A. J. van Soest, M. E. Roebroeck, M. F. Bobbert, P. A. Huijing, G. J. van Ingen Schenau, 1985. A comparison of one-legged and two-legged countermovement jumps. Med. Sci. Sports Exerc. 17(6):635-9.

Kelly S. Hale and Kay M. Stanney, 2004, Deriving HapticDesign Guidelines from Human Physiological, Psychophysical, and Neurological Foundations, IEEE

Roland Sigrist & Georg Rauter & Robert Riener & Peter Wolf, Augmented visual, auditory, haptic, and multimodal feedback in motor learning: A review, Psychonomic Society, Inc. 2012

Laura Marchal-Crespo*1 and David J Reinkensmeyer Review of control strategies for robotic movement training after neurologic injury, Journal of NeuroEngineering and Rehabilitation 2009, 6:20

Yeong-Hwa Chang, Yung-Te Chen, Chia-Wen Chang, Chih-Lung Lin Development scheme of haptic-based system for interactive deformable simulation, Computer-Aided Design 42 (2010) 414424

David Feygin1, Madeleine Keehner2, Frank Tendick2 Haptic Guidance: Experimental Evaluation of a Haptic Training Method for a Perceptual Motor Skill 2002 IEEE

Increased movement accuracy and reduced EMG activity as the result of adopting an external focus of attention Tiffany Zachry a, Gabriele Wulf a,∗, John Mercer a, Neil Bezodis b , Brain Research Bulletin 67 (2005) 304–309

Hogan and Buerger Impedance and Interaction Control, 2005

Hogan, An impedance control, 1985

Head Coordination as a Means to Assist Sensory Integration in Learning to Walk, BLANDINE BRILa,c,* AND ANNICK LEDEBTb,c, Neuroscience and Biobehavioral Reviews, Vol. 22, No. 4, pp. 555–563, 1998

The sensorimotor and cognitive integration of gravity, Thierry Pozzo a,), Charalambos Papaxanthis a, Paul Stapley a, Alain Berthoz b, 1998

Changes in Otolith VOR to Off Vertical Axis Rotationin Infants Learning to Walk Preliminary Results of a ongitudinal Study"S. R. WIENER-VACHER,b A. LEDEBT?.' AND B. BRIL', 1996

SLIP Running with an Articulated Robotic Leg Marco Hutter, C. David Remy, Mark A. Höpflinger, and Roland Siegwart, Fellow, IEEE 2010

Websites:

eksobionics.com

rewalk.com

rexbionics.com

novint.com

bit-tech.net

https://msdn.microsoft.com/en-us/library/hh874757.aspx

Appendix A

Code, data and protocols are found at the link:

https://drive.google.com/folderview?id=0B11MXMNostcEfjNaZENDZG9SVGdhdVFyU254dWx3bkU3LUpnWktYODB5QWtwTkdOWF80WVU&usp=sharing